

This is the peer reviewed version of the following article:

The Messinian salinity crisis in the Adriatic foredeep: Evolution of the largest evaporitic marginal basin in the Mediterranean / Manzi, V.; Argnani, A.; Corcagnani, A.; Lugli, S.; Roveri, M.. - In: MARINE AND PETROLEUM GEOLOGY. - ISSN 0264-8172. - 115:(2020), pp. 1-19. [10.1016/j.marpetgeo.2020.104288]

Terms of use:

The terms and conditions for the reuse of this version of the manuscript are specified in the publishing policy. For all terms of use and more information see the publisher's website.

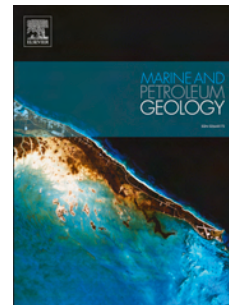
14/12/2025 08:23

(Article begins on next page)

Journal Pre-proof

The Messinian salinity crisis in the Adriatic foredeep: Evolution of the largest evaporitic marginal basin in the Mediterranean

V. Manzi, Argnani A, Corcagnani A, Lugli S, Roveri M



PII: S0264-8172(20)30071-4

DOI: <https://doi.org/10.1016/j.marpetgeo.2020.104288>

Reference: JMPG 104288

To appear in: *Marine and Petroleum Geology*

Received Date: 13 June 2019

Revised Date: 26 December 2019

Accepted Date: 7 February 2020

Please cite this article as: Manzi, V., A, A., A, C., S, L., M, R., The Messinian salinity crisis in the Adriatic foredeep: Evolution of the largest evaporitic marginal basin in the Mediterranean, *Marine and Petroleum Geology* (2020), doi: <https://doi.org/10.1016/j.marpetgeo.2020.104288>.

This is a PDF file of an article that has undergone enhancements after acceptance, such as the addition of a cover page and metadata, and formatting for readability, but it is not yet the definitive version of record. This version will undergo additional copyediting, typesetting and review before it is published in its final form, but we are providing this version to give early visibility of the article. Please note that, during the production process, errors may be discovered which could affect the content, and all legal disclaimers that apply to the journal pertain.

© 2020 Published by Elsevier Ltd.

CRediT author statement

Manzi Vinicio: Conceptualization, Methodology, Investigation, Writing - Original Draft, Writing - Review & Editing, visualization, Supervision.

Argnani Andrea: Conceptualization, Investigation, Writing - Original Draft, Writing - Review & Editing

Corcagnani Alessandro: Investigation, Writing - Original Draft, Writing - Review & Editing

Lugli Stefano: Conceptualization, Methodology, Investigation, Writing - Original Draft, Writing - Review & Editing

Roveri Marco: Conceptualization, Methodology, Investigation, Writing - Original Draft, Writing - Review & Editing

The Messinian salinity crisis in the Adriatic foredeep: evolution of the largest evaporitic marginal basin in the Mediterranean

Manzi V., Argnani A., Corcagnani A., Lugli S., Roveri M.

ABSTRACT

The recent release of a large number of subsurface geological data by the Italian Minister of Economic Development, including boreholes and seismic profiles, provided the occasion for a new assessment of the deposits associated with the Messinian salinity crisis (MSC) in the Adriatic foreland basin system and a new integration with the outcropping successions of the Apennines. In particular, the study of the Messinian evaporites allowed to reconstruct a new detailed palaeogeographic and palaeobathymetric framework for all the stages of the crisis.

We identified the largest evaporitic marginal basin ever described for the Mediterranean hosting the precipitation of the primary shallow-water gypsum deposits (PLG, Primary Lower Gypsum) during the first stage of the crisis. During the second and third stages of the crisis, the PLG basin underwent uplift and erosion and the evaporite accumulation moved to the deeper part of the basin and was characterized by the deposition of the Resedimented Lower Gypsum unit including clastic evaporites, recycling the PLG ones, primary halite and terrigenous deposits.

The distribution of the different evaporitic facies, was the basis for an improved reconstruction of the upper Miocene tectonic evolution of the Apennines thrust belt. Our results show a clear separation between shallower depocenters, located in the wedge-top and in the Adriatic foreland basins and characterized by MSC stage 1 PLG deposition, and deeper-water ones, located in the Adriatic foredeep and close to the Calabrian Arc, where MSC stage 2 terrigenous and gypsum-bearing clastic deposits and primary halite accumulated.

1. INTRODUCTION

The distribution of the Messinian salinity crisis (MSC) related deposits in the Apennines and in the Adriatic foredeep basin has been matter of several studies during the last decades, mostly based on outcrop data (Roveri et al., 2001, 2004, 2006, 2014b).

33 Recently, the Ministry of Economic Development of Italy (*MISE, Ministero dello Sviluppo*
34 *Economico*), through the project entitled “Visibility of petroleum exploration data in Italy”
35 (*ViDEPI, Visibilità dei dati afferenti all'attività di esplorazione petrolifera in Italia*) has
36 released a large amount of subsurface data filed since 1957 and covering the whole Italian
37 territory. The ViDEPI database includes a large number of boreholes and industrial seismic
38 profiles for hydrocarbon investigation. All the boreholes and the seismic lines can be
39 accessed and downloaded for free at the ViDEPI website
40 (<http://www.videpi.com/videpi/videpi.asp>) or through the Arcgis platform
41 (<https://arcg.is/1vXmrl>). A great part of these boreholes crossed the Messinian deposits,
42 especially in the offshore areas. Their analyses made it possible to recognize the
43 subsurface equivalents of the deposits cropping out in the Apennines and to provide a
44 detailed reconstruction of the distribution of the MSC-related deposits all along the
45 Apennines foredeep.

47 **2. THE MESSINIAN SALINITY CRISIS (MSC): A BRIEF OVERVIEW**

48 The Messinian salinity crisis (MSC; 5.97-5.33 Ma) is one of the more dramatic
49 palaeoceanographic and biological event in the Earth's history, during which huge
50 volumes of evaporites accumulated on the Mediterranean seafloor because of the reduced
51 connections with the Atlantic Ocean, due to the interplay between tectonic uplift in the
52 Gibraltar area and glacio-eustatic changes (Krijgsman et al., 1999). The largest part of the
53 evaporites deposited during the MSC is now buried below the deep Mediterranean
54 seafloor but the large number of outcrops has allowed the reconstruction of a very-high
55 resolution stratigraphic framework through the integration of bio-, magneto- and
56 cyclostratigraphic data (Clauzon et al., 1996; Krijgsman et al., 1999; Hilgen et al., 2007;
57 CIESM, 2008). Although a detailed distribution of the MSC deposits in the offshore area
58 has been made available (Lofi et al., 2011; Lofi, 2018), the lack of continuous cores and
59 logs in the deeper settings together with insufficient seismic resolution leave the
60 interpretation of the different seismic facies still a problematic issue (see discussion in
61 Roveri et al., 2019).

62 **2.1 MSC stages**

63 A large consensus has been reached during the last decade by the scientific community
64 in subdividing the MSC into three evolutionary stages, each of them well time-constrained
65 and characterized by peculiar evaporite deposits and palaeohydrological conditions

66 (CIESM, 2008; Roveri et al., 2014a,b). Controversies still persist on what actually occurred
67 during these three stages, especially for what concerns the variations of the
68 Mediterranean sea level.

69 **Stage 1 (5.97-5.60 Ma)** - According to Roveri et al. (2008; 2019) and Lugli et al. (2010),
70 shallow-water (< 200m) bottom-grown primary evaporites (PLG, Primary Lower Gypsum;
71 accumulated only in marginal silled basins, whereas organic- and dolomite-rich
72 foraminifer-barren shales sedimented in deeper water (Manzi et al., 2007; FBI, Foraminifer
73 Barren Interval, *sensu* Manzi et al., 2018). Up to 16 shale-gypsum cycles were deposited
74 under a strong astronomical control to form up to 200 m-thick evaporite successions (Vai,
75 1997; Hilgen et al., 2007; Lugli et al., 2010). According to other authors, based on the
76 interpretation of seismic data, PLG deposition also occurred in deeper waters (Ochoa et
77 al., 2015) or was replaced by halite (Meilijson et al., 2018, 2019).

78 **Stage 2 (5.60-5.55 Ma)** - It represents the crisis acme. The marginal basins that hosted
79 the PLG deposition during stage 1 underwent uplift and deep erosion. In this stage
80 evaporite deposition shifted to the deeper settings and was characterized by both clastic
81 (derived from the dismantlement of the PLG unit) and primary evaporites (cumulate
82 deposits of gypsum, halite and K-Mg salts) deposits, grouped into the Resedimented
83 Lower Gypsum unit (RLG; Roveri et al., 2008a). The connections with the Atlantic were
84 further reduced but still sufficient to allow accumulation of marine water-derived salt. This
85 stage was marked by a widespread tectonic activity and by a sea level drop, which is still
86 lively debated in terms of timing (before, during or after halite deposition; see discussion in
87 Roveri et al., 2014b) and magnitude (from 100-200 m; according to Roveri et al., 2016;
88 Manzi et al., 2018; up to 800 m according to Druckman et al., 1995; 800-900 m for the
89 Adratic basin, Amadori et al., 2018; up to more than 1500 m according to Lofi et al., 2005;
90 Bache et al., 2009).

91 **Stage 3 (5.55-5.33 Ma)** - This is the last and probably the less known stage of the
92 crisis. The deposition of primary evaporites was limited to the southern and eastern portion
93 of the Mediterranean Sea (Sicily, Cyprus, Crete) and completely absent in the Apennines
94 foredeep. The peculiar Lago-Mare fossil associations, including hypohaline mollusk,
95 ostracod and dinocyst (Rouchy et al., 2001; Bertini, 2006; Orszag-Sperber et al., 2006;
96 Cosentino et al., 2007; 2012; Gliozzi et al., 2007; Grossi et al., 2008; Pellen et al., 2017,
97 Roveri and Manzi, 2006; Roveri et al., 2008c; Ruggieri, 1967), suggests the development
98 of hypohaline conditions possibly related to the input of Paratethyan water in the
99 Mediterranean basin. However, on the basis of the occurrence of marine fossils (fishes;

100 Carnevale et al., 2006; dinocysts, Popescu et al., 2009; Pellen et al., 2017; long-chain
101 alkenones, Vasiliev et al., 2017), possible oceanic incursions during the last stage of the
102 crisis have been envisaged (Bache et al., 2009; 2012). Marine waters may have provided
103 the ions needed for the precipitation of the Upper Gypsum evaporites during insolation
104 minima (Manzi et al., 2009). Depleted Sr isotope values and the increased terrigenous
105 deposits during this stage point to a Mediterranean Sea characterized by hypohaline
106 waters, more humid climatic conditions and enhanced fresh-water input (Roveri et al.,
107 2014a,b). The recognition of the peculiar Sr signature in both shallow and deep settings
108 (Roveri et al., 2014a; Gvirtzman et al., 2017; Manzi et al., 2018) suggests the persistence
109 of water connections between the Mediterranean subbasins also during the stage 3 that
110 were likely filled by a unique water body. However, other authors hold that, at least at the
111 beginning of stage 3, the Mediterranean basin was almost desiccated, based on the
112 occurrence of inferred fluvial deposits above the stage 2 halite in the Levantine Basin
113 (Madof et al., 2019).

114

115 **2.2 MSC surfaces**

116 This MSC stratigraphic framework is based on the recognition of some key-surfaces
117 (Roveri et al., 2019; and their Fig. 3):

118 **onset surface (OS)** – It marks the crisis onset placed in the 4th precessional cycle above
119 the Gilbert chron at 5.97 Ma (Manzi et al., 2013). It is associated with the sudden
120 disappearance of the foraminifers. It can be found indistinctively at the base of the PLG
121 unit or at the base of the FBI (Manzi et al., 2007; 2018);

122 **evaporites onset surface (EOS)** - It is a diachronous surface flooring the PLG, only
123 locally coinciding with the OS; The Messinian deposits laying above the EOS belongs to
124 stage 1 and are younger than 5.97 Ma;

125 **Messinian erosional surface (MES \equiv base of the p-ev₁ unit)** - It is a widespread
126 unconformity surface (Cita and Corselli, 1990) locally associated with angular discordance
127 and local subaerial exposure (Vai, 1988). It can be traced from the top of the PLG unit in
128 the marginal basins up to the base of the RLG unit in the deep ones. It has been
129 recognized offshore along the Mediterranean basin margin (Ryan and Cita, 1978; Lofi et
130 al., 2005; Roveri et al., 2014b and references therein). In the deeper portion of the basins
131 the MES pass to its correlative conformity surface (MES-cc; Roveri et al., 2008b; 2019).
132 The deposits laying above the MES belongs to stage 2 or 3 and are always younger than

133 5.60 Ma; this surface marks the dismantlement of the PLG deposits and their
134 re sedimentation in the foredeep lows (Roveri et al., 1998; 2006; 2008c).
135 **ash layer (al)** – A rhyolitic volcanoclastic key-bed dated at 5.53 Ma (Roveri et al., 1998;
136 Trua et al., 2010; Cosentino et al., 2013) found in the whole Adriatic foredeep and locally
137 in Calabria and Sicily, roughly marking the base of stage 3, is often found at the top of the
138 RLG unit;
139 **base of p-ev₂** – dated at 5.42 Ma, this surface can be regarded as a maximum regressive
140 surface for the MSC succession (Roveri et al., 2008b) marking a change from regressive
141 to transgressive trend in the post-evaporitic succession. In the marginal settings this
142 surface commonly is found at the base of fluvio-deltaic deposits, whereas, in deeper
143 settings, it marks the base of coarser-grained turbiditic deposits. Above this surface a
144 higher diversity hypohaline biota is commonly present (“Lago-Mare” *sensu stricto*; Roveri
145 et al., 2008c).
146 **Miocene/Pliocene or Messinian/Zanclean boundary (M/P)** – this surface marks the
147 Messinian-Zanclean boundary placed at 5.33 Ma, 5 precessional cycles below the base of
148 the Thvera magnetic event (Van Couvering et al., 2000) and marked by the return to fully
149 marine conditions in the Mediterranean; in the Apennines, it is commonly associate with a
150 black shale organic-rich horizon (Roveri et al., 2006).

151

152 3. GEOLOGICAL SETTING

153 The study area includes different portions of the Apennines that have been historically
154 considered as worlds apart. We try here to limit the Apennines subdivision into two main
155 paleogeographic domains, autochthonous and allochthonous that were deposited
156 respectively in the outer and in the inner portion of the Apennines fold and thrust system.
157 We focus on the late Miocene-early Pliocene terms of the stratigraphic succession (Fig. 1).

158 3.1 Autochthonous domains

159 All the sedimentary successions deposited in basins resting on the undeformed portions of
160 the foredeep and foreland above Adria and Apula that experienced only minor tectonic
161 translations after the MSC are grouped in this domain.

162 3.1.1 Northern Apennines

163 The northern area includes the foredeep basin formed above the Umbro-Marchean
164 units characterized by a thick Triassic-Jurassic shallow water carbonate succession
165 (Burano Anhydrites, Calcare Massiccio, Calcari a Posidonia, Rosso Ammonitico units)

166 followed by Cretaceous-Paleogene hemipelagic carbonate and marls (Maiolica, Fucoidi
167 marls, and Scaglia Fms). While the inner Umbro-Marchean unit (Fig. 1a) was involved in
168 the Apennines orogenesis, the outer Umbro-Marchean unit (Fig. 1a) was characterized,
169 since the Langhian, by the deposition of a thick Alpine-derived siliciclastic fill extending for
170 hundreds of km along the Adriatic foredeep from the Emilia-Romagna to the Umbria region
171 (Ricci Lucchi, 1986; Argnani and Ricci Lucchi, 2001).

172 During the late Tortonian an important tectonic phase affecting the whole Apennines
173 caused the eastward migration of the foredeep (Ricci Lucchi, 1986), the formation of the
174 Vena del Gesso wedge-top basin (VdG; Roveri et al., 2003) and the segmentation of the
175 main foredeep into minor basins (Eastern Romagna; Northern Marche; Laga; Fig. 1).

176 In the inner sectors of the foredeep, affected by tectonic segmentation, turbidite
177 deposition stopped during the late Tortonian while their deposition continued during the
178 whole MSC and in the Pliocene in the undeformed foredeep (e.g. the Laga basin; Ricci
179 Lucchi, 1975; 1986). The turbidites were deposited in the more subsiding portions of the
180 Adriatic foredeep. Conversely, in wedge-top basins or in the foreland ramp, that were not
181 reached by the turbiditic flows moving along the foredeep axis, the pre-MSC succession
182 commonly consists of hemipelagic deposits (Euxinic shale and Schlier Formations),
183 showing a well-developed cyclic pattern given by the alternation of sapropels, marls and
184 diatomite, the deposition of which is strictly controlled by variation of Earth orbital
185 parameters (Vai, 1997; Krijgsman et al., 1999). These deposits are characterized by a
186 large fossiliferous content (foraminifers, nannofossils, and locally mollusks); their
187 sedimentation rate is quite reduced as the last 1.2-1.5 Ma preceding the crisis onset have
188 been recorded by less than 50-60 m (Manzi et al., 2007; 2018).

189 The sub-basins of the foredeep were characterized by different stratigraphies. During
190 stage 1, the primary evaporites (PLG) were deposited only in shallow basins, like the
191 thrust-top VdG basin (Roveri et al., 2003) and in the foreland (Roveri et al., 1986; 1992;
192 2005; Rossi et al., 2015); in the deeper basin of the Romagna and Marche this interval is
193 characterized by the deposition of an organic-rich and dolomite-rich foraminifer-barren
194 shale unit (FBI; Manzi et al., 2007; 2018). During stage 2, the VdG basin was uplifted, the
195 PLG unit was eroded and resedimented in the adjoining basins to form the RLG unit
196 (Manzi et al., 2005). The stage 3, in this sector, is characterized by the absence of
197 evaporites and by the deposition of Apennine-derived terrigenous deposits (San Donato,
198 Colombacci, Laga units; Bassetti et al., 1994; Ricci Lucchi, 1975; 1986; Ricci Lucchi et al.,
199 2002; Roveri et al., 2001; Milli et al., 2007) containing peculiar hypohaline biota and

200 showing strong thickness variability, from few meters in the VdG basin up to more than 1
201 km in the deeper buried portions of the foredeep (Fusignano Fm; Cremonini and Ricci
202 Lucchi, 1982). The return to the fully marine conditions at the base of the Zanclean was
203 sharp and marked by a black, organic-rich horizon (Roveri et al., 2004; 2006).

204 The outer Umbro-Marchean unit is limited to the south by the Gran Sasso thrust front
205 involving the carbonate units of the Lazio-Abruzzi platforms, the front of the Molise-
206 Lagonegro nappe, and is bounded to the east by the Apulian Platform, including the
207 Gargano high (G; in red in Fig. 1a) that originated mostly in the Late Miocene-Pliocene
208 (Argnani et al., 2009).

209 In the most elevated portions of the Lazio-Abruzzi platform, the carbonate deposition
210 continued until the salinity crisis. In the Maiella area the *Lithothamnion* limestone facies,
211 representing the younger term of the Bolognano Fm., was deposited until the lower
212 Messinian (Brandano et al., 2012; Cornacchia et al., 2017); in its upper part, this unit
213 passes gradually to marl deposits containing *T. multiloba*, whose distribution zone (6.34-
214 5.97 Ma; Sierro et al., 2001; Manzi et al., 2007) is quite close to the onset of the MSC.
215 Around the Gargano high, on top of the Apula platform, the pre-MSC late Miocene
216 succession is incomplete and poorly age-constrained; it includes shallow water limestone
217 deposits (breccias and calcarenites), the deposition of which is supposed to have been
218 continued until the early Messinian. No evaporites crop out in this area. The pre-crisis unit
219 is capped unconformably by the Gravina calcarenites, a Pliocene unit which age is not
220 strongly constrained.

221 Moving southward, the Messinian deposits of the outer Umbro-Marchean unit continue into
222 the Bradanic Trough, as shown by boreholes and seismic data, although their place into
223 the stratigraphic framework is still lacking. These deposits are buried under the
224 allochthonous Molise-Lagonegro Nappe, which was emplaced during the Plio-Pleistocene
225 (Patacca and Scandone, 2007; 2011).

226

227 **3.2 Far-travelled Allochthonous domains**

228 This domain includes all the semiallochthonous geological terranes that during the late
229 Miocene were located in the more inner (western) position of the foredeep and that during
230 the Plio-Pleistocene translated in their present position above the Autochthonous domains
231 (Fig. 1).

232 **3.2.1 Northern Apennines**

233 In the Northern Apennines the Emilia and the Val Marecchia Epiligurian units were
234 deposited over a late Jurassic-lower Eocene Ligurian complex translating (north)eastward
235 over the Tuscany and Umbro-Marchean-Romagna domains. These Epiligurian satellite
236 basins are characterized by Messinian successions similar to those of the VdG basin
237 (Manzi, 2001; Gennari et al., 2013), with thick PLG unit eroded on top and sealed by the
238 uppermost portion of the Lago-Mare unit and by the Pliocene marine clay unit. The PLG
239 lays conformably on a shelf shale succession (Termina, Ca' i Gessi formations; Ruggieri,
240 1970; Roveri et al., 1999; Gennari et al., 2013) the base of which is locally marked by late
241 Tortonian sandstones (Termina Fm) and conglomerates (Acquaviva Fm), in the Emilia and
242 in the Val Marecchia, respectively. During the Messinian the Epiligurian basins were
243 located in a more internal position with respect to the VdG basin; they reached their
244 current position during the middle Pliocene.

245 3.2.2 Southern Apennines

246 In the southern Apennines two main translated domains can be distinguished: the
247 Molise and Lagonegro nappe and the Calabrian Arc.

248 The Molise-Lagonegro Nappe (Fig. 1) represents the accretionary wedge of the
249 Calabrian Arc (e.g., Argnani, 2005; Casero, 2004; Vitale and Ciarcia, 2013) and consists
250 of a Triassic-lower Miocene tectonic complex including slabs of deep basinal (shale and
251 cherty limestone) and flyschoid deposits (carbonate or siliciclastic turbidites). These units
252 are capped by a relatively less deformed late Miocene-early Pliocene succession (Matano
253 et al., 2005); it is formed by i) a pre-MSC unit including the Faeto flysch and Toppo-
254 Capuana marls; ii) an evaporite unit (Monte Castello Fm) capped by terrigenous unit
255 (Anzano molasse, Torrente Fiumarella unit) and by the Pliocene shallow marine to deltaic
256 deposits (Ariano unit). The evaporites crop out discontinuously but they are well exposed
257 in three localities, Cervaro River, Monte Ferrara and Scampitella quarries (Matano et al.,
258 2007) where, on the basis of gypsum facies (massive, banded and branching selenite) and
259 Sr signature (within stage 1 range) an incomplete succession, up to 50 m-thick, can be
260 recognized. The base of the PLG is poorly exposed but is assumed to be conformable.
261 Conversely, its top is unconformable and overlain by terrigenous deposits containing
262 scarce hypohaline ostracods and mollusks that can be assigned to the stage 3. A reduced
263 succession is found in the outer portion of the Molise allochthonous both in outcrop and
264 subsurface, including blocks of PLG unconformably capped by the Lago-Mare deposits
265 (Cosentino et al., 2018).

266 The Calabrian Arc (Van Dijk, 2000; Fig. 1) consists of pre-Triassic metamorphic and
267 intrusive units in places with Alpine metamorphism, originally located close to Corsica-
268 Sardinia, were translated south-eastward because of the opening of the Tyrrhenian Sea
269 since the late Tortonian (e.g., Argnani 2005; Cipollari et al., 1999; Kastens et al., 1988).
270 The Ionian side of the Calabrian Arc is characterized by a late Miocene-Pleistocene
271 succession resting unconformably on the crystalline basement and its Mesozoic-Cenozoic
272 sedimentary cover, or on the Mesozoic-Paleogene terrigenous units accreted in front of
273 the Calabrian Arc (Van Dijk, 2000; Roveri et al., 2008; Zecchin et al., 2003). The MSC
274 units rest on a late Tortonian-early Messinian marine unit consisting of thin-bedded
275 turbidites, marl and diatomite (Ponda Formation) resting in turn on a fluvio-deltaic
276 conglomerates succession (San Nicola unit) derived from the dismantlement of the
277 crystalline and metamorphic basement. In the Crotona and Rossano basins the deposits
278 consist of a lower clastic carbonate and gypsum deposits (Roveri et al., 2008a; Manzi et
279 al., 2011), belonging to the RLG unit, that rest unconformably above the pre-crisis units
280 and are floored by the MES. Locally an organic-rich evaporitic-free unit barren of
281 foraminifers, representing the deep time-equivalent of the stage 1 evaporites, is preserved
282 (Roveri et al., 2008d). Above the resedimented gypsum unit a hybrid (gypsum, carbonate
283 and siliciclastic) unit including halite lenses is present (detritico-salina unit; Roda, 1964), in
284 turn capped by a fluvio-deltaic unit with Lago-Mare faunal associations including
285 conglomerate lenticular bodies (Carvane unit, Roda, 1964). The end of the crisis is marked
286 by the deposition of lower Pliocene open marine marls (Cavaliere marls) followed by the
287 siliciclastic deposits of the Belvedere Fm (Roda, 1964; Van Dijk, 2000).

288

289 **4. METHODS**

290 In this work we have considered 1341 boreholes belonging to the offshore zones of the
291 Adriatic and Ionian Sea (offshore zones A, B, D, F in the ViDEPI database) and the
292 onshore Autochthonous Domain. An extended version of the methods is provided in the
293 supplementary document. Among the 1341 boreholes:

- 294 - 642 do not cross the MSC units because are drilled in younger or older deposits;
- 295 - 363 do not cross the MSC interval because of an erosional hiatus; in the supplementary
296 documents (tab. S1 and klm file), these boreholes are grouped on the basis of the pre-
297 crisis unit ages;

298 - 336 cross the MSC; in the supplementary documents (tab. S1 and klm file), these
299 boreholes are grouped according to the crossed evaporite deposits.
300 We focused of the late Tortonian-early Pliocene stratigraphic interval in order to
301 reconstruct the distribution of the deposits associated with the Messinian salinity crisis
302 along the Adriatic foredeep.
303

304 **5. THE OUTCROPPING MSC UNITS**

305 Here we will briefly describe the main physical and sedimentological characters of the
306 different evaporitic units as they appear in outcrop; these features can be useful in the
307 interpretation of the borehole logs.

308 **5.1 Primary bottom-grown gypsum (PLG unit; stage 1)**

309 Due to its peculiar characters the PLG unit is easily recognizable in the field. The
310 complete succession forms large-scale tabular bodies with a thickness of 200 m or more
311 (Fig. 2a,b) and includes up to 16 gypsum beds separated by thin (typically 1-3 m) intervals
312 of dark euxinic shales (Fig. 3a). The internal organization, which is maintained over large
313 distances, is characterized by (Lugli et al., 2010; Fig. 3a): i) two lowermost thin (<10m)
314 gypsum beds (PLG1-2) with giant crystals massive selenite showing a lateral transition to
315 limestone (Manzi et al., 2013); ii) three intermediate very thick (up to 35 m) and very lateral
316 persistent gypsum beds (PLG3-5) with massive and banded selenite facies; iii) up to 11
317 thick (10-15 m) gypsum bed (PLG6-16) showing the presence of branching selenite in the
318 upper part of the beds. Despite the variation in absolute thickness, the relative thickness of
319 the gypsum beds remains rather constant in the different basins and the presence of the
320 intermediate cluster formed by the thickest beds (PLG3-5; Fig. 13 in Lugli et al., 2010; Fig.
321 2b, 3a) can be easily identified, thus, representing a key horizon useful for stratigraphic
322 correlations.

323 The gypsum facies, are characterized by a different resistance to weathering with a
324 characteristic erosional profile. The PLG1-5 gypsum beds being made up by massive
325 coarse and interlocked gypsum crystals (massive and banded facies) with sharp upper
326 and lower boundaries. The gypsum beds of the upper cycles (PLG6-16) may show
327 relatively smoother tops due to the presence of the more erodible branching selenite
328 facies containing a larger amount of limestone and/or shale (Fig. 3b).

329 The PLG deposits rest conformably on hemipelagic or shelf shale and are erosionally
330 cut at the top by the MES.

331 **5.2 Gypsum and hybrid clastic deposits (RLG unit; stage 2)**

332 The RLG unit is floored by the MES; it rests unconformably on pre-crisis deposits but
333 locally, in the basinal areas where the MES pass down basin to its correlative conformity
334 surface (MES-cc), a barren organic-rich shale interval (FBI) is present below the unit
335 (Manzi et al., 2007). The RLG evaporites form tens of m-thick lenticular or tabular bodies
336 (Fig. 2c) characterized by a great variability of clastic facies that can be grouped as follows
337 (Manzi et al., 2005; 2011).

338 **5.2.1 Mass wasting gypsum-bearing deposits (RLG1)**

339 This group includes mass-wasting deposits, submarine glides, slides and slumps,
340 cohesive flows (facies R0, R1 of Manzi et al., 2005). These deposits include heterometric
341 PLG-derived gypsum block and chaotic shale. They are characterized by individual
342 lenticular beds, with irregular bases and tops, forming wedge-shape bodies close to the
343 main tectonic slopes, e.g. the large slope complex found close to the structural high
344 bounding the VdG basin (Roveri et al., 2003) similar PLG-bearing chaotic bodies emplaced
345 during the stage 2 of the crisis are described in seismic also at the front of the Ligurian
346 nappe close to Reggio Emilia (Rossi et al., 2002) and in the Cortemaggiore wedge-top
347 basin (Artoni et al., 2007).

348 **5.2.2 gypsum-bearing turbidites (RLG2)**

349 This group includes the gypsum-bearing gravity flow deposits (granular flows and high- to
350 low-density turbidity currents; facies R2 to R7 of Manzi et al., 2005) commonly consisting
351 of m-thick composite graded beds showing a lower coarser-grained (rudite or arenite)
352 gypsum-bearing division capped by a finer-grained one mostly composed by gypsiltite or
353 shale (Fig. 3c). Commonly these beds show a good lateral persistency and limited
354 thickness (Fig. 2c). Carbonate and terrigenous sandstone clasts recycled from older
355 deposits may be found in the coarser-grained interval. The base of these beds is
356 commonly sharp and the top is smooth due to the normal gradation and the transition to
357 the shale interval.

358 **5.3 Primary halite and gypsum deposits (RLG unit; stage 2)**

359 These deposits can only be observed where diapirs crop out or in mines in Calabria
360 (Crotona basin), Sicily (Caltanissetta basin) and Tuscany (Volterra basin) otherwise they
361 are absent in the rest of the Apennines. Halite forms lenticular bodies with local thickness
362 up to 600 m due to intense halotectonics. Internally they consist of dm-thick beds
363 separated by thin anhydrite or shale horizons; thin K-Mg rich salt beds are locally found in
364 the middle part of the halite bodies (Lugli et al., 1999; Manzi et al., 2012).

365 **5.4 post evaporitic deposits (Lago-Mare unit; stage 3)**

366 The primary gypsum deposits of the Upper Gypsum unit (UG; Manzi et al., 2009) occur
367 only in the Caltanissetta basin (Sicily), capping the RLG unit. In the Calabrian arc and in
368 the rest of the Apennines the RLG is capped by thick terrigenous fine-grained deposits
369 including a rhyolitic volcanoclastic key-bed described in paragraph 2 and showing a
370 coarser-grained upper portion (p-ev₂ unit) including conglomerates (Cusercoli Fm,
371 Romagna, Roveri et al., 1998, 2006; Carvane unit, Crotone basin, Calabria, Roda, 1964),
372 sandstones and thin limestone layers (so called colombacci). The Lago-Mare biota are
373 mostly distributed in the p-ev₂ unit and in its time equivalent, upper half, portion of the
374 Upper Gypsum unit. The end of the crisis is marked everywhere by the sudden transition
375 to fully marine deposits, commonly preceded by a dark shale horizon (Roveri et al., 2006).

376 **6.CRITERIA FOR THE LOG INTERPRETATION OF THE MSC UNITS IN THE** 377 **SUBSURFACE**

378 The 1341 boreholes drilled in the study area can be grouped as follows on the basis of
379 the crossed deposits (see tab. S1):

380 *Boreholes not crossing the MSC* - 642 boreholes did not cross the salinity crisis
381 deposits because drilled within younger or older deposits. The latter have been useful in
382 the definition of the extension of the Allochthonous terrains

383 *Boreholes with hiatus including the MSC* - In 363 boreholes the crisis interval is
384 represented by an erosional hiatus of variable amplitude. For those boreholes where the
385 late Tortonian-early Messinian is present, the recognition of shelf carbonates,
386 hemipelagites and turbidites allows a rough distinction between shallow vs. deep pre-MS
387 deposits.

388 *Boreholes crossing the MSC* - The Messinian interval has been crossed in 336
389 boreholes. In this case, a first distinction is based on the presence or absence of evaporitic
390 deposits. A further distinction is based on the different characteristics of evaporitic
391 deposits.

392 The different lithologic units belonging to the late Tortonian-early Pliocene interval
393 crossed by the boreholes have been distinguished on the basis of their typical
394 characteristics observed from the geophysical logs, gamma ray (GR), resistivity (RES) and
395 sonic (Δt) as reported in in tab. S2. First, the evaporites can be easily distinguished from
396 the siliciclastic and hemipelagic deposits not only directly (cuttings analysis) but also
397 indirectly on the basis of geophysical logs especially for the higher resistivity, lower Δt and

398 lower gamma-ray (with the exception of the K-Mg salts). Then, among the evaporites a
399 further distinction between primary gypsum, clastic gypsum and halite deposits can be
400 obtained on the basis of the different values and vertical pattern observed in the gamma
401 ray, resistivity and sonic logs.

402 A main subdivision includes three main group of rocks.

403 **6.1 Evaporite-free intervals**

404 These intervals consist mostly of clay or marl deposits containing minor sandstone or
405 carbonate horizons devoid of evaporites. The intervals are commonly characterized by
406 very low ($<10 \Omega\text{m}$) resistivity, relatively high gamma ray (50-100 API units) and Δt (60-200
407 $\mu\text{s}/\text{ft}$). The presence of sandstone or carbonate can be highlighted by small increase of
408 resistivity and decrease of gamma ray and Δt . The pattern of geophysical logs has
409 commonly a monotonous trend, local spikes are recorded where thin sand or carbonate
410 layers are crossed.

411 **6.2 Gypsum-rich intervals**

412 Gypsum-rich intervals are characterized by high resistivity (200-600 Ωm), low gamma
413 ray (0-10 API units) and low Δt (45-50 $\mu\text{s}/\text{ft}$). Among them the primary deposits (PLG) can
414 be easily distinguished from the clastic ones (RLG) based on the log patterns:

415 **6.2.1 Primary Lower Gypsum intervals (PLG)**

416 The PLG unit is characterized by a peculiar blocky pattern obtained by thin spikes of
417 low resistivity/high gamma ray that punctuate a high resistivity/low gamma ray base line,
418 that reflect the lithological composition of the succession (Lugli et al., 2010; Sampalmieri et
419 al., 2008; 2010). These features allow the recognition and count of the cycles from the
420 geophysical logs that can be used for stratigraphic correlations. In particular the typical
421 stacking pattern can be recognized from logs (e.g. Patrizia_001, Fiona_001, Morgia_001
422 boreholes; Fig. S1): two thin ($< 10 \text{ m}$) lowermost cycles (PLG1-2), three very thick and
423 massive cycles (PLG3-5) and up to 11 medium (10-15 m) cycles (PLG-6-16). In the
424 geophysical logs, PLG-1-5, consisting of massive and banded selenite facies only, show
425 commonly both sharp bases and tops, whereas PLG-6-16 beds, due to the presence of
426 the branching selenite, may show a sharp base but a smoother top.

427 **6.2.1 Resedimented Lower Gypsum intervals (RLG)**

428 The RLG unit (e.g. Thurio_001 and Dalila_001 boreholes; Fig. S1) is characterized by a
429 (finely) spiky pattern obtained from a thin alternation of spikes with high resistivity/low
430 gamma ray (gypsum) and spikes with low resistivity/high gamma ray (clays). As shown in
431 the previous paragraph the clastic gypsum beds are thinner with respect to the PLG beds.

6.3 Salt-rich intervals

A very high resistivity (~10000 Ohm.m) identifies the salt-rich interval (e.g. Thurio_001 borehole; Fig. S1). The alternation of thin halite, gypsum and clay may result in a spikey pattern whereas massive halite may produce a blocky one. Halite is commonly characterized by low gamma ray values (0-10 API units) whereas K-salts can be highlighted by higher values (100-200 API units). Δt is commonly low (60-75 $\mu\text{s}/\text{ft}$).

7. RESULTS

7.1 Reconstruction of the Adriatic evaporitic basin

The boreholes used in this work are those crossing the salinity crisis interval represented by sediments or by hiatus. Two main groups can be distinguished (Fig. 4a): *The Adriatic foreland units* - These deposits resting on the Autochthonous Domain and covered by the Plio-Pleistocene succession are found in the more external domains that were only partially involved in the Apennine deformation, the foredeep and foreland ramp basins (below the Adriatic Sea).

In the Southern Apennines these units include deposits that rest on the Autochthonous Domain (Fig. 1b), and in particular on the Apulian Platform domain, but are tectonically overlain by the units of the Translated domains. The Adriatic foredeep and foreland units have been found in the Southern Apennines and were reached below the Molise-Lagonegro Nappe allochthonous units. The post-MSC succession is absent or reduced because of the allochthonous thrusting above the MSC units; it becomes progressively more complete toward the external zones on the foredeep, allowing the reconstruction of Far-travelled Allochthonous domains migration during the Pliocene (Patacca and Scandone, 2007; Bigi et al., 2013).

Translated MSC units – These deposits resting on the Far-travelled Allochthonous and covered by the Plio-Pleistocene succession are found in the buried basins of the Calabrian Arc and in the north-eastern portion of the Molise-Lagonegro Nappe.

A reconstruction of the early Tortonian-Messinian stratigraphy obtained by the analysis of the boreholes data is here proposed separated into three time intervals (Fig. 4 b,c,d):

Pre-MSC (Tortonian-Messinian; 8.50-5.97 Ma; Fig. 4b)

The large part of the pre-MSC deposits of the Autochthonous Domain is characterized by the deposition of fine-grained (marls and sapropels) hemipelagic deposits whereas the deposition of the Tortonian-Messinian siliciclastic turbidites is limited to the western portion

465 of the northern Apennines foredeep and in the outer Marnoso-arenacea and Laga basins.
466 Shelf carbonate deposits are found in a small area extending in a WNW-ESE direction
467 from the Gran-Sasso-Maiella area to the northern Gargano (between Pescara and
468 Foggia). Interbedded hemipelagic and shelf terrigenous deposits (clays with sandstone
469 lobes) were deposited in the eastern basins of the Calabrian Arc (Roda, 1964; Roveri et
470 al., 1992).

471 Stage 1 (5.97-5.60 Ma; Fig. 4c)

472 During the first stage the deposition of the PLG unit is limited to: i) the wedge-top basins
473 of the Autochthonous Domain, ii) the wedge top basins translating above the Ligurian and
474 Molise-Lagonegro nappes and ii) to the Adriatic foreland basins (Fig. 1).

475 The best example in the wedge-top basins of the Autochthonous domains is found in
476 the Vena del Gesso basin (Roveri et al., 2003) where the reference section for the
477 evaporites of the stage 1 is present (Monte Tondo section; Lugli et al., 2010). In the
478 satellite basins developed above the allochthonous units, three main areas can be
479 distinguished: Marecchia river valley, Irpinia and Molise. In the Marecchia river valley
480 (Gennari et al., 2013) and in Irpinia (Matano et al., 2005) the PLG unit rests conformably
481 above a pre-MSC shelfal shale succession. Conversely in the Molise area Cosentino et al.
482 (2018), having observed that the PLG unit rests indistinctly above the Varicolored Clays
483 (Cretaceous-Paleogene) or the Faeto flysch (Aquitania-lower Messinian) deposits,
484 suggested the presence of an unconformity at its base. In the area south-west of Termoli,
485 between the Saccione and the Trigno rivers, 13 boreholes crossed an evaporite unit that
486 can be assigned to PLG on the basis of the analogies in term of thickness and trend of the
487 geophysical logs with that drilled a few km to the north resting above the Autochthonous
488 Domain. It is worth noting that 5 out of the 13 boreholes reached the PLG on the top of the
489 Apulian succession below the allochthonous units. As correctly reported by Cosentino et
490 al. (2018) the PLG above the Molise-Lagonegro Nappe is commonly found resting above a
491 clayey succession of not well-defined age. However, considering that the PLG unit crops
492 out in small isolated blocks at the front of the Molise-Lagonegro Nappe (e.g. Stingeti and
493 Gessaro; Cosentino et al., 2018) and that it is present in the foreland below the Molise-
494 Lagonegro Nappe, a different interpretation could be suggested. The PLG could have
495 been accreted at the front of the Molise-Lagonegro Nappe when the allochthonous units
496 translated over the foreland, where the unit rests conformably above the AD; in this view
497 the base of the PLG cannot be considered an unconformity.

498 The Adriatic foreland succession is characterized by a main depocenter located in the
499 Adriatic offshore between the Gargano and the Conero Riviera (Ori et al., 1986; Roveri et
500 al., 2005; Corcagnani, 2017). Here, several boreholes crossing the PLG unit allowed the
501 reconstruction of 6 correlation panels (Fig. 5) and 4 isopach maps (Fig. 6).

502 The PLG commonly overlays hemipelagic deposits, but in the Gran-Sasso-Maiella area
503 it rests above shelf carbonates developed since the early Miocene; thus, suggesting the
504 presence of shallow-waters environment well before the MSC onset. In the other areas no
505 PLG are found. Based on outcrop (Northern Apennines, Manzi et al., 2007; Conero
506 Riviera, Iaccarino et al., 2008; Calabria, Roveri et al., 2008d) and subsurface data in the
507 Northern Adriatic foredeep (Rossi et al., 2015) an organic-rich, dolomitic-rich, foraminifers-
508 barren shale unit can be found in the area where the PLG unit is absent (Fig. 4b).

509 The peculiar pattern of the PLG successions observed in outcrops and described in the
510 previous paragraphs, allows the recognition in the offshore of the individual cycles from
511 boreholes. The correlations between the boreholes showing the best geophysical logs
512 (see Fig. 5) have been traced along three NW-SE-oriented panels (sections 1, 2 and 3)
513 and three panels perpendicular to the previous ones (sections 4, 5 and 6) in order to show
514 the internal variations of the unit. The cluster formed by the thickest cycles, PLG3-5, can
515 be easily recognized; it is continuous all along the sections providing a helpful tool for
516 stratigraphic correlations. The lowermost cycles PLG1-2 have been detected in several
517 sections; thus, confirming the conformable character of the base of the PLG. Conversely,
518 the unit appears truncated on top by the MES and sealed by the Lago-Mare or directly by
519 the Pliocene deposits; the latter become younger eastward, as described in the Conero
520 area (Ori et al., 1986; Roveri et al., 1986; 2005). Because of this upper truncation the
521 entire succession is rarely preserved. The most complete successions are found in the
522 southern area (Morgia-001 dir, Bomba-001 and Fontemaggiore-002 dir boreholes) where
523 up to 16 cycles can be recognized.

524 The analysis of the variation of the thickness of individual beds can be performed for the
525 lower cycles only. In fig. 6 it is possible to appreciate the variation of the thickness of
526 PLG1+2, PLG3 and PLG4, each one up to 40 m-thick. The thickness decreases
527 northward, close to the Abruzzo coastline where the Apulian platform deepens
528 (Santantonio et al., 2013; Trincardi et al., 2011c) below the Pescara basin (Ori et al.,
529 1986), filled in mostly during the Plio-Pleistocene. Unfortunately, no boreholes are
530 available in this area and thus it is possible to follow the PLG further to the west only on
531 the ViDEPI seismic lines (e.g. B-415, B-416, B-417, B-418, B-439, B-440 from ViDEPI; the

532 subsurface map in Trincardi et al., 2011c) and thus no data on the internal organization of
533 the evaporites can be inferred. In the Conero Riviera (Roveri et al., 1986; 2005) the unit
534 ends eastward against a structural high that has been subsequently incorporated in the
535 Conero thrusts. In general, it is possible to recognize a decrease in thickness of the beds,
536 in section 2, in the western-central part of the basin. Conversely, the larger thicknesses
537 are mostly found in the southeastern part. This suggest that the bed thickness is
538 decreasing with the paleodepth as suggested by Lugli et al. (2007; 2010).
539 Close to the Adriatic midline, the cycles remain relatively thick. Unfortunately, no boreholes
540 are available beyond the midline, and consequently it is not possible to see how the
541 thickness of the unit and of its individual beds vary further eastward.

542 The lateral continuity of the PLG is deduced from the seismic profiles and from the
543 geological maps available for the Adriatic offshore (Roveri et al., 2005; Trincardi et al.,
544 2001; 2011a-e; Corcagnani, 2017) that show the absence of major tectonic structures and
545 an almost horizontal bedding. It follows that the thickness obtained from the boreholes can
546 be used for the reconstruction of the isopach maps (Fig. 6b, c, d). The PLG1+2 beds are
547 relatively thin and have been grouped together. PLG3 and PLG4 have been considered in
548 separate maps. No map has been reconstructed for the overlying beds because they are
549 not continuous all along the study area due to erosion at the top.

550 The preservation of the complete succession in the southwestern area between the Gran
551 Sasso and the Gargano can be explained in terms of evolution of the foredeep. During the
552 pre-MSC this area was shallow, and shelf carbonate deposits accumulated, while
553 hemipelagic deposits were deposited more to the north. During stage 2 and later this area
554 experienced a rapid subsidence that can be related to the flexure of the foreland ramp due
555 to the load of the eastward migrating Apennine chain; thus, the present-day depth of the
556 PLG unit has been reached long after their deposition.

557 The upper cycles are characterized by a slightly attenuated log response with respect to
558 the PLG3-5 cycles. This can be related to the presence of branching selenite facies that
559 contains shale and/or limestone, making the upper portion of the upper cycles, less
560 resistant to the erosion with respect to the lower cycles. These differences may have
561 implications in the production of the resedimented evaporites after the erosion of the PLG
562 unit; the upper cycles are more suitable to provide sand-sized detritus whereas the lower
563 cycles provide more easily large blocks (Manzi et al., 2005). We infer that the erosion of
564 the upper cycles may have provided a detritus with a grain-size suitable to be transported
565 and redeposited by turbiditic flows in the deeper portion of the foredeep.

566 Stage 2+3 (5.60-5.33 Ma; Fig. 4d)

567 These two stages are considered together because the stratigraphic resolution of the
568 logs does not allow to define with precision the boundary between the two stages.

569 During stage 2 the previously deposited PLG unit were eroded and resedimented in the
570 deeper portions of the foredeep (Marche and Laga basins), in the Bradanic Through and in
571 the wedge-top basins of the Calabrian Arc.

572 In general, the resedimented gypsum present at the base of the MSC succession and
573 resting unconformably above Tortonian-early Messinian shale deposits can be assigned to
574 stage 2. The presence of halite lenses intercalated with clastic gypsum has been
575 recognized only in boreholes drilled above the allochthonous units of the Calabrian Arc
576 (fig. 4d). The only exception is found in a small area in the Basilicata region, described
577 below.

578 Evaporite-free deposits containing typical hypohaline biological association are
579 comprised between the clastic evaporites, below, and the Pliocene, above, and can be
580 assigned to stage 3. The Lago-Mare biota could be present also in the stage 2 deposits
581 but become more abundant in stage 3 (Roveri et al., 2008c); the direct recognition in
582 boreholes indicate a relatively high abundance of biota, suggesting an assignment to
583 stage 3 rather than to stage 2.

584 **7.2 The Messinian Apennines: distribution of the MSC deposits**

585 The distribution of the different evaporitic facies in the Adriatic foredeep led to depict
586 more clearly the geological evolution of the Apennines during and after the MSC. The
587 integration of outcrop and borehole data has been the base for the reconstruction of two
588 borehole-based regional-scale geological sections (Fig. 7) extending from the Tyrrhenian
589 to the Adriatic sides of the Apennines.

590 A geological section (Fig. 7a) extending S-N from the Salerno gulf up to the Central
591 Adriatic Sea shows the relationships between the Allochthonous units of the Apennine
592 orogenic wedge and the Autochthonous Domain. According to the boreholes stratigraphy,
593 along this section the Far-travelled Allochthonous domains is a tectonic accretionary
594 complex consisting of undifferentiated Miocene deposits including varicolored shale
595 (Sicilids), quartzarenite (Numidian Flysch), cherty limestone, late Tortonian-early Miocene
596 marls and minor thin layers of clastic gypsum and carbonate. The precipitation of the
597 primary bottom-grown gypsum during the stage 1 occurred in the more elevated structural
598 settings: in the piggy-back basins above the northeastward moving Molise-Lagonegro

599 Allochthonous units and in the Adriatic foreland (Matano et al., 2005; Roveri et al., 2005).
600 The boreholes that reached the Autochthonous Domain below the Molise-Lagonegro
601 Nappe show that the deposition of the PLG is limited to an area located to the north (fig. 1)
602 characterized by pre-MSC shallow water carbonate deposits. This structural elevated area
603 on the Apula Platform, here called “palaeogargano” and mostly corresponding with the
604 Gargano-Pelagosa paleo sill of Pellen et al., 2017, was located close to the present-day
605 Gargano high (G fig. 6a) and confined the Adriatic PLG basin to the south. To the north of
606 the sill a large Adriatic evaporitic basin hosted the deposition of the PLG (Fig. 4c), from the
607 Termoli area (Guglionesi 001 borehole) up to Adriatic midline (Bora 001 borehole) and
608 even more to the east.

609 Moving south of the “palaeogargano sill” the MSC deposits disappear for a 50 km-long
610 tract where the Mesozoic carbonates are deeply eroded and capped by Pliocene deposits.
611 In order to find other Messinian deposits, it is necessary to move more to the south, where
612 PLG evaporites are absent and only clastic evaporites of the RLG unit have been reached
613 by boreholes crossing the whole Molise-Lagonegro Nappe (from Montestillo 001 to Taurasi
614 001).

615 The W-E section (Fig. 7b), perpendicular to the previous one, shows more clearly the
616 large subsidence experienced by Apula under the load of the Allochthonous units, where
617 the RLG units are capped by up to 200 m of Lago-Mare deposits (Bellaveduta 001). It is
618 worth noting the direct fault system that lowered the western side of Apula in the Bradanic
619 Trough. The section reports the Irpinia basin where the PLG accumulated, on top of the
620 Allochthonous units. Conversely, below the TA, only clastic evaporites are present (from
621 Bellaveduta 001 to Taurasi 001). The zoom of the allochthonous front, in fig. 7c, shows the
622 deformations of Apula and the stratigraphic hiatus below the Pliocene deposits.

623 A slightly different situation can be described for the Basilicata area (Fig. 8). Here the
624 evaporites, consisting of clastic gypsum and/or halite (Recoleta 001, Cavone Bernalda
625 001, S. Basilio 001) are found in the allochthonous units overthrusting the late Pliocene
626 marine deposits. No evaporites are found directly above the Mesozoic carbonates of Apula
627 that are unconformably covered by Pliocene deposits, which are progressively younger
628 (from early to upper Pliocene) moving from Letizia 001 to F. Basento 001). The Messinian
629 evaporites can thus be considered here as foredeep units accreted at the front of the
630 Molise-Lagonegro Nappe as they have been deposited more to the west and at a greater
631 depth than their present-day location.

632 We have also reconstructed two regional-scale seismic sections in the northern and
633 central Apennines (Fig.9) in order to better show the distribution of the evaporites in the
634 Adriatic foreland. In the northern Apennines (Fig. 9a) we have reconstructed a seismic
635 section, extending in a SSW-NNE direction from the Vena del Gesso Basin to the Adriatic
636 foreland in the Veneto area, by integration of two published seismic sections (section 5 of
637 Fantoni et al., 2010; section SL-1 of Roveri et al., 2003). The PLG deposits are limited to
638 the more elevated positions, in the wedge-top VdG basin, where they crop out, and in the
639 foreland only in a limited portion beyond the more external thrust involving the Mesozoic
640 succession with its hangingwall anticline is now located below the city of Ferrara.
641 Conversely, the more subsiding area saw the deposition of a thick terrigenous turbidites
642 unit (Fusignano Fm; Cremonini and Ricci Lucchi, 1982), that includes resedimented
643 gypsum deposits at its base, laying unconformably above the late Tortonian-early
644 Messinian deposits or, in the deeper portion of the foredeep, conformably above an
645 organic- and dolomitic-rich shale interval representing stage 1 (PLG time-equivalent
646 deposits; Manzi et al., 2007; Rossi et al., 2015).

647 In the central Apennines we have reconstructed a second seismic section (Fig. 9c) that
648 integrating two published sections (fig. 1b of Bigi et al., 2011; fig. 6 of Wrigley et al., 2015)
649 and 5 seismic lines available from the ViDEPI database (Fig. 9b). In this section it is
650 possible to appreciate the great extension of the Adriatic evaporitic units. The integration
651 of seismic and borehole data allows to recognize the conformable base and the
652 unconformable top of the evaporitic unit eroded by the MES. In the eastern side, the PLG
653 unit is limited by a deep thrust belonging to the external Dinaric front and involving the
654 more external portions of the Mesozoic carbonate platform and the Oligo-Miocene
655 succession; more eastward the MSC units are no longer present. Moving to the western
656 termination of the PLG basin a change in the seismic geometries is observed across a
657 thrust fault few km west of the Dante_001 borehole. Beyond this structure the reflector
658 marking the base of the PLG is lacking and the MES cuts down to the pre-MSC units and
659 is onlapped by post-evaporitic deposits which become older to the west up to include the
660 late Messinian terms of the Laga Formation (stage 2 and 3). Gypsum-clastic deposits
661 (indicated with G in Fig. 9b) are found in boreholes at the base of this MES-floored post-
662 evaporitic unit. The MSC units become thicker moving further to the west, in the
663 depocenter of the Laga basin where a 2500-3000 m-thick turbiditic unit was deposited
664 during the whole Messinian (Bigi et al., 2009; Artoni, 2003); around 700 m of this unit was
665 deposited during the post-evaporitic interval (stage 2+3).

666

667 **8. DISCUSSION**

668 **8.1. Implication for tectonic reconstructions**

669 The distribution of the evaporites provides some important constraints that can be used
670 for the restoration of the Apennines in the Messinian.

671 A first constraint comes from the presence of the MSC deposits below the Molise-
672 Lagonegro Nappe, which implies a restoration of the allochthonous front up to 100 km to
673 the south (fig. 7a) and to the west (fig. 7b), thus a minimum total retreat of the front of the
674 Molise-Lagonegro Nappe up to 65 km to the SW.

675 A second important constraint comes from the PLG distribution. At present time the
676 elevation of the PLG above the allochthonous domains reach more than 750 m above sea
677 level in the Irpinia basins, and around 100 m in the Biferno Valley (Cosentino et al., 2018).
678 In the Adriatic offshore the PLG are at different depths varying from almost 2 km below
679 sea level in the south part of the basin and around 800-1000 m in the northern one. Since
680 the deposition of the PLG occurred in photic environment in shallow water basins (<200 m
681 according to Lugli et al., 2010), it is possible to reconstruct the palaeobathymetry of the
682 different sectors. This allows to reconstruct the vertical movements that affected the
683 different sectors of the Apennines. For instance, the Irpinia basin have been uplifted of
684 more than 900 m since the PLG time, likely because of the overthrusting of the Molise-
685 Lagonegro nappe above the Apula Platform; the latter, due to the load of the
686 Allochthonous domains subsided rapidly more than 1500 m.

687 Integrating published paleotectonic reconstructions (Argnani, 2005; 2013; Vai, 2016)
688 with the constraints obtained from the distribution of the MSC deposits we can outline a
689 palaeogeographical reconstruction that account for the depositional environments during
690 the salinity crisis (see the paleogeographic map in Fig. 10).

691 The paleogeographic map refers to the stage 2 of the MSC, but also includes the
692 location of the PLG (stage 1) in order to show the relationships between the shallow
693 depositional areas of PLG that represent the source of the clastic evaporites deposited in
694 the deeper basins (e.g. Apennine foredeep and deep wedge top basins) during stage 2, as
695 described below.

696 To appreciate the contribution of the detailed Messinian stratigraphy and facies analysis
697 three main steps in the evolution of the Apennines can be considered.

698 Pre-MSC (8-5,97 Ma)

699 This interval is very important to understand the evolution of the Apennines because it
700 includes an important phase of tectonic reorganization of the Mediterranean area that is
701 marked by the widespread deposition of coarser grained siliciclastic deposits (Fontanelice
702 member of the Marnoso-arenacea, Fm Northern Apennines, Ricci Lucchi, 1975; Roveri et
703 al., 2003; Laga Fm., Central Apennines, Ricci Lucchi, 1975.; S. Nicola dall'Alto
704 conglomerates, Calabria, Roda, 1974; Terravecchia Fm, Sicily, Ruggieri and Torre, 1984)
705 followed by a phase of tectonic quiescence that preceded the onset of the crisis and that is
706 characterized by the predominant deposition of hemipelagic (Schlier, Tripoli, euxinic
707 shales Fms) and, locally, shelf carbonate deposits (Fig. 4).

708 Stage 1 (5.97-5.60 Ma)

709 This interval is characterized by the deposition of PLG deposits in shallow-water (<200
710 m; Lugli et al., 2010), silled basins formed in the fold-and-thrust belt (wedge-top basins)
711 and possibly in the foreland (Figs. 4, 10). Compared with the other Mediterranean areas
712 where the unit crops out, the Adriatic basin is much larger (see comparison in tab. S1).
713 Additional smaller occurrences of PLG deposits above the foreland, are found in basins
714 located both onshore (EV basin) and offshore (between Ravenna and the Po river delta)

715 All these basins containing PLG can be considered to have an average paleo water-
716 depth of 100 m. At the same time, in the deeper poorly oxygenated portion of the basins
717 an organic-rich barren shale unit is found in the northern Apennines (Manzi et al., 2007),
718 Calabria (Roveri et al., 2008d), Sicily (Manzi et al., 2011) and in the Tyrrhenian (Roveri et
719 al., 2014a), Piedmont (Dela Pierre et al., 2011), and Levant basins (Manzi et al., 2018)

720 Stage 2+3 (5.60-5.33 Ma)

721 After stage 1, a new important tectonic phase possibly enhanced by a sea level drop,
722 for which magnitude, timing and duration are still debated (see paragraph 2.1 MSC
723 stages), was responsible for the incision of the PLG deposits and their re-sedimentation in
724 the topographic lows via gypsum-bearing slides, olistostromes and turbidity currents. This
725 time interval is also characterized by strong evaporation, possible related to a further
726 restriction of the connections with the Ocean, testified by the accumulation of a large
727 volume of halite in the deepest depocenters. All these evaporites, resting on the MES, are
728 included in the RLG unit (Roveri et al., 2008a). What really happened in this phase is a
729 highly controversial point in the MSC debate. However, one of the proposed scenarios
730 envisaging that increased evaporation led to the formation of halite-saturated brines in
731 shallow-water settings which moved as density currents toward the deeper basins of the
732 Mediterranean (Roveri et al, 2014c), fits well with the observations in the study area. It is

733 worth noting, in fact, that halite has not been found in situ above the Apulian Platform, but it
734 is present in some sectors of the Calabrian Arc (e.g., the Crotona basin), in those areas that
735 were deeper during the pre-MSC and stage 1 (Figs. 4, 10). Following this interpretation, a
736 thick halite unit was deposited in the deep Ionian basin and in its western sector. The
737 halite unit was subsequently accreted at the front of the Calabrian Arc during the south-
738 eastward migration of the arc that occurred in the Plio-Quaternary (e.g. Gutsher et al.,
739 2017).

740 In the Apennine outcrops the RLG unit is overlain by thick terrigenous deposits
741 (Fusignano, San Donato, Colombacci, Laga, Carvane Fm) including the typical brackish
742 Lago-Mare biological association in its upper part. Notably, in Sicily, this interval is
743 characterized by the deposition of the Upper Gypsum deposits.

744 During the uppermost Messinian, the Apennine foredeep has been sometimes considered
745 to be segmented in small perched basins (Bache et al. 2012, Pellen et al., 2017 and
746 reference therein), completely isolated from the Mediterranean by the Gargano-Pelagosa
747 sill. On the contrary, in our reconstruction (Fig. 10) the Adriatic and Ionian water masses
748 were connected, although the depocentral part of the Apennine foredeep (during stage 2)
749 was confined to the south by the allochthonous units that were encroaching the Apulian
750 Platform. Our analysis of the ViDEPI dataset allows to define a large area (pink area in
751 Fig. 04 d) where the evaporites are buried below the Molise-Lagonegro Nappe (Fig. 7). On
752 the basis of log patterns, the unit can be interpreted as clastic evaporites (RLG), similar to
753 those extending from the Romagna to the Laga basin (Manzi et al., 2005). Conversely, the
754 evaporites found above the Molise-Lagonegro Nappe belong to the PLG, deposited during
755 stage 1.

756 Therefore, it can be inferred that the Molise-Lagonegro Nappe during stage 1 was close to
757 sea level, because of its thrusting onto the Apulian Platform. On the contrary, the stage 2
758 deposits in the Crotona basin, resting above the allochthonous units, indicate a deep water
759 depositional environment.

760 The black arrows in Fig. 10 are intended to illustrate the inferred routing of clastic
761 sediments, without implying a precise path. The same applies to the red arrows that depict
762 possible flow paths of salt brine feeding the deep basin, coming from the adjacent shallow
763 marine areas where the brine factories are inferred to be located. The slopes of the halite
764 basins are studded by canyons (e.g. Lofi, 2018) which can act as potential fairways for the
765 clastic gypsum turbidites and the salt brines.

766 It is worth noting that borehole data do not allow to reconstruct the high-resolution
767 stratigraphic framework for the stage 3 which was obtained from the outcropping
768 successions. It follows that, the distribution of the Lago-Mare sediments below the Molise-
769 Lagonegro Nappe can not be defined.

770

771 **8.2. The distribution of the PLG deposits at the Mediterranean scale**

772 Another important output derived from the analysis of the evaporite deposits in the
773 Mediterranean is represented by the reconstruction of the area where the PLG deposits
774 accumulated during the first stage of the crisis. The area where these evaporites have
775 been preserved from erosion in the Adriatic and Emilia shallow foreland settings (Fig. 1)
776 can be estimated to be $\sim 30'000 \text{ km}^2$.

777 A comparison with the other PLG basins in the Mediterranean, taking a rough calculation
778 based on the present-day PLG distribution from literature (Tab. S1), suggests that the
779 areal extent of the deposits in the Adriatic region may have been greater than the sum of
780 all the other PLG basins of the entire Mediterranean, which is about $45'000 \text{ km}^2$. The
781 occurrence of such a large area of PLG deposition can be related to the tectonic setting
782 that provided a large shallow-water basin isolated from the main clastic supplies of Alpine
783 and Apennines provenance, which accumulated in the deeper foredeep settings.
784 Moreover, the preservation of the PLG deposits was favored by the subsidence that
785 affected the Adriatic foreland after stage 2, related to the load of the eastward migrating
786 Apennine thrust belt.

787 **9. CONCLUSIONS**

788 After the public release of the subsurface data obtained for hydrocarbons investigations
789 in Italy, a large number of boreholes and seismic data have been made available. The
790 analyses and the integration of these data allowed to reconstruct with an unprecedented
791 detail the distribution of the MSC evaporites and evaporite-free deposits and the evolution
792 of the Apennines chain. The main conclusions of our work are:

- 793 - during stage 1 the deposition of the evaporites was limited to the marginal basins
794 located in the Apennines wedge-top and foreland;
- 795 - the Adriatic foreland basin represents the largest evaporitic marginal basin of the
796 Mediterranean ever described;
- 797 - in the Adriatic foreland the PLG unit rests conformably above hemipelagites or
798 shallow-water carbonates;

- 799 - the geophysical logs allow to recognize and count the evaporite cycles from the
800 boreholes, providing a 3D reconstruction of the PLG succession;
- 801 - the thicker, more complete and better preserved PLG successions are located in the
802 western portion of the Adriatic basins; their preservation was favored by the
803 subsidence due to the foreland flexure induced by the progressive load of the
804 Apennine orogen during the Plio-Pleistocene;
- 805 - the PLG unit is truncated on top by the MES, which is in turn sealed by the latest
806 Messinian Lago Mare deposits or by the Pliocene;
- 807 - the MES can be followed from the top of the PLG unit toward the base of the Late
808 Messinian-early Pliocene succession; clastic gypsum deposits are locally found
809 above it;
- 810 - in the deeper portion of the Apennine foredeep (central and northern Apennines)
811 gypsum is a minor component of the siliciclastic turbidite fill;
- 812 - within the orogenic edifice, the halite deposition is limited to small satellite basins
813 above the Calabrian Arc (Basilicata area, Crotona basin) where it is associated to
814 clastic gypsum.
- 815 - the distribution of the evaporites provides an estimation of the vertical and horizontal
816 movements that affected the Autochthonous and Allochthonous settings of the
817 Apennines thrust-belt and foreland system after the MSC.
- 818

819 **ACKNOWLEDGMENTS.**

820 Journal Editor (M. Zecchin), Associate Editor (F. Bache) and three anonymous
821 reviewers are greatly acknowledged for their useful suggestions that let us to greatly
822 improve the earlier version of the manuscript.

823 **REFERENCES**

- 824 Amadori, C., Garcia-Castellanos, D., Toscani, G., Sternai, P., Fantoni, R., Ghielmi, M., Di
825 Giulio, A., 2018. Restored topography of the Po Plain-Northern Adriatic Region during
826 the Messinian baselevel drop - implications for the physiography and
827 compartmentalization of the paleo-Mediterranean basin. Basin Research. doi:
828 10.1111/bre.12302
- 829 Argnani, A., 2000. The Southern Apennines-Tyrrhenian System within the kinematic of the
830 Central Mediterranean. Mem. Soc. Geol. It., 55, 112-122.

- 831 Argnani, A., 2005. Possible record of a Triassic ocean in the southern Apennines.
832 *Bollettino della Società Geologica Italiana*, 124, 109-121.
- 833 Argnani, A., 2009. Evolution of the southern Tyrrhenian slab tear and active tectonics
834 along the western edge of the Tyrrhenian subducted slab. *Geological Society of*
835 *London, Special Publications* 311, 193-212.
- 836 Argnani, 2013. The role of Mesozoic palaeogeography in the evolution of the Southern
837 Apennines. *Rend. Online Soc. Geol. It.*, 25, 11-20.
- 838 Argnani, A., Ricci Lucchi F., 2001. Tertiary silicoclastic turbidite systems of the Northern
839 Apennines, 327-349. In Vai G.B and Martini I.P. Eds. "Anatomy of an Orogen: The
840 Apennines and Adjacent Mediterranean Basins" Springer.
- 841 Artoni, A., 2003. Messinian events within the tectono-stratigraphic evolution of the
842 Southern Laga Basin (Central Apennines, Italy). *Boll. Soc. Geol. It.*, 122, 447-465.
- 843 Artoni, A., Rizzini, F., Roveri, M., Gennari, R., Manzi, V., Papani, G., Bernini, M., 2007.
844 Tectonic and Climatic Controls on Sedimentation in Late Miocene Cortemaggiore
845 Wedge-Top Basin (Northwestern Apennines, Italy). In: Lacombe O., Lavé J., Roure F.,
846 Vergés J. (Eds.) *Thrust belts and Foreland Basins. From fold kinematics to hydrocarbon*
847 *systems*. Springer.
- 848 Bache, F., Olivet, J.-L., Gorini, C., Rabineau, M., Baztan, J., Aslanian, D., Suc, J.-P., 2009.
849 Messinian erosional and salinity crisis: view from the Provence basin (Gulf of Lions,
850 western Mediterranean). *Earth and Planetary Science Letters* 286, 139–157.
- 851 Bache, F., Popescu, S.M., Rabineau, M., Gorini, C., Suc, J.P., Clauzon, G., Olivet, J.L.,
852 Rubino, J.L., Melinte-Dobrinescu, M.C., Estrada, F., Londeix, L., Armijo, R., Meyer, B.,
853 Jolivet, L., Jouannic, G., Leroux, E., Aslanian, D., Reis, A.T.D., Mocochain, L.,
854 Dumurdžanov, N., Zagorchev, I., Lesić, V., Tomić, D., Namik Çağatay, N., Brun, J.P.,
855 Sokoutis, D., Csato, I., Uçarkus, G., Çakir, Z., 2012. A two-step process for the
856 reflooding of the Mediterranean Basin after the Messinian Salinity Crisis. *Basin*
857 *Research* 24, 125-153.
- 858 Barone, M., Critelli, S., Le Pera, E., Di Nocera, S., Matano, F., Torre, M., 2006:
859 *Stratigraphy and Detrital Modes of Upper Messinian Post-evaporitic Sandstones of the*
860 *Southern Apennines, Italy: Evidence of Foreland-Basin Evolution during the Messinian*
861 *Mediterranean Salinity Crisis*. *International Geology Review*, 48, 702–724.
- 862 Bassetti, M.A., Ricci Lucchi, F., Roveri, M., 1994. Physical stratigraphy of the Messinian
863 post-evaporitic deposits in Centralsouthern Marche area (Apennines, Central Italy).
864 *Mem. Soc. Geol. Ital.* 48, 275–288.
- 865 Bertini, A., 2006. The Northern Apennines palynological record as a contribute for the
866 reconstruction of the Messinian palaeoenvironments. *Sedimentary Geology* 188/189:
867 235-258.

- 868 Bigi, S., Moscatelli, M., Milli, S., 2009. The Laga basin: Stratigraphic and Structural
869 Setting. *Geol.F.Trips*, 1, 50-27
- 870 Bigi, S., Casero, P., Ciotoli, G., 2011. Seismic interpretation of the Laga basin; constraints
871 on the structural setting and kinematics of the Central Apennines. *Journal of the*
872 *Geological Society of London*, 168, 179-190.
- 873 Bigi, S., Conti A., Casero, P., Ruggiero L., Recanati, R., Lipparini, L., 2013. Geological
874 model of the central Periadriatic basin (Apennines, Italy). *Marine and Petroleum*
875 *Geology*, 42, 107-121.
- 876 Boccaletti, M., Ciaranfi, N., Cosentino, D., Deiana, G., Gelati, R., Lentini, F., Massari, F.,
877 Moratti, G., Pescatore, T., Ricci Lucchi, F., Tortorici, L., 1990. Palinspastic restoration
878 and paleogeographic reconstruction of the peri-Tyrrhenian area during the Neogene.
879 *Palaeogeography, Palaeoclimatology, Palaeoecology*, 77, 41- 50.
- 880 Brandano, M., Lipparini, L., Campagnoni, V., Tomassetti, L., 2012. Downslope-migrating
881 large dunes in the Chattian carbonate ramp of the Majella Mountains (Central
882 Apennines, Italy). *Sedimentary Geology* 255-256, 29-41.
- 883 Carnevale, G., Landini, W., Sarti, G., 2006. Mare versus Lago-mare: marine fishes and the
884 Mediterranean environment at the end of the Messinian Salinity Crisis. *Journal of the*
885 *Geological Society of London* 163, 75–80.
- 886 Casero, P., 2004. Structural setting of petroleum exploration plays in Italy. In: Crescenti,
887 U., d'Offizi, S., Merlino, S., Sacchi, L. (Eds.), *Geology of Italy. Special Publication of the*
888 *Italian Geological Society for the IGC 32nd*. Florence, 2004, pp. 189-199.
- 889 Cornacchia, I., Andersson, P., Agostini, S., Brandano, M., Di Bella, L., 2017 Strontium
890 stratigraphy of the upper Miocene Lithothamnion Limestone in the Majella Mountain,
891 central Italy, and its palaeoenvironmental implications. *Lethaia*, 50, 561-575.
- 892 CIESM, 2008. The Messinian salinity crisis from mega-deposits to microbiology. A
893 consensus report. In: Briand, F., Monaco (Eds.), *33ème CIESM Workshop*
894 *Monographs*, 33, 91-96.
- 895 Cipollari, P., Cosentino, D., and Gliozzi, E., 1999. Extension- and compression-related
896 basins in central Italy during the Messinian Lago-Mare event: *Tectonophysics*, 315,
897 163–185.
- 898 Cita, M.B., Corselli C., 1990. Messinian paleogeography and erosional surfaces in Italy: an
899 overview. *Palaeogeography, Palaeoclimatology*, 77-1, 67-82. Clauzon, G., Suc, J.P.,
900 Gautier, F., Berger, A., Loutre, M.F., 1996. Alternate interpretation of the Messinian
901 salinity crisis, controversy resolved? *Geology*, 24, 363–366.
- 902 Corcagnani, A., 2017. La Crisi di salinità del Messiniano nell'avampaese Adriatico:
903 ricostruzione delle relazioni tra successioni onshore e offshore attraverso lo studio di
904 log di pozzo e sismica industriale (Database ViDEPI).

- 905 Cosentino, D., Gliozzi, E., Pipponzi, G., 2007. The late Messinian Lago-Mare episode in
906 the Mediterranean Basin: preliminary report on the occurrence of Paratethyan ostracod
907 fauna from central Crete (Greece). *Géobios*, 40: 339-349.
- 908 Cosentino, D., Bertini, A., Cipollari, P., Florindo F., Gliozzi, E., Grossi, F., Lo Mastro, S.,
909 Sprovieri, M., 2012. Orbitally forced paleoenvironmental and paleoclimate changes in
910 the late postevaporitic Messinian of the central Mediterranean Basin. *GSA Bulletin*, 124-
911 3/4, 499–516.
- 912 Cosentino, D., Buchwaldt, R., Sampalmieri, G., Iadanza, A., Cipollari, P., Schildgen, T.F.,
913 Hinnov, L.A., Ramezani, J., Bowring, S.A., 2013. Refining the Mediterranean
914 “Messinian gap” with high-precision U-Pb zircon geochronology, central and northern
915 Italy. *Geology*, 41, 323-326.
- 916 Cosentino, D., Bracone, V., D'Amico, C., Cipollari, P., Esu, D., Faranda, C., Frezza, V.,
917 Gliozzi, E., Grossi, F., Guerrieri, P., Iadanza, A., Kotsakis, T., Soulié-Märsche, I., 2018.
918 The record of the Messinian salinity crisis in mobile belts: Insights from the Molise
919 allochthonous units (southern Apennines, Italy). *Palaeogeography, Palaeoclimatology,*
920 *Palaeoecology*, 503, 112-130.
- 921 Cremonini, G., and Ricci Lucchi, F. ,1982. Guida alla geologia del margine appenninico
922 padano. Guide Geologiche regionali della Società Geologica Italiana. Bologna.
- 923 Dela Pierre, F., Bernardi, E., Cavagna, S., Clari, P., Gennari, R., Irace, A., Lozar, F., Lugli,
924 S., Manzi, V., Natalicchio, M., Roveri, M., Violanti, D., 2011. The record of the
925 Messinian salinity crisis in the Tertiary Piedmont Basin (NW Italy): the Alba section
926 revisited. *Palaeogeography, Palaeoclimatology, Palaeoecology* 310, 238–255.
- 927 Druckman, Y., Buchbinder, B., Martinotti, G.M., Tov, R.S., Aharon, P., 1995. The buried
928 Afiq Canyon (eastern Mediterranean, Israel): a case study of a Tertiary submarine
929 canyon exposed in Late Messinian times: *Marine Geology*, 123, 167-185.
- 930 Fantoni, R., Franciosi R., 2010. Tectono-sedimentary setting of the Po Plain and Adriatic
931 Foreland. *Rend. Fis. Acc. Lincei*, 21/1, S197–S209
- 932 Fantoni, R., Decarlis A., Fantoni E., 2003. L'estensione mesozoica al margine occidentale
933 delle Alpi Meridionali (Piemonte Settentrionale, Italia). *Atti Ticinensi di Scienze della*
934 *Terra*, 44, 97–110.
- 935 Fauquette, S., Bertini, A., Manzi, V., Roveri, M., Argnani, A., Menichetti, E., 2015.
936 Reconstruction of the Northern and Central Apennines (Italy) palaeoaltitudes during the
937 late Neogene from pollen data. *Review of Palaeobotany and Palynology*, 218, 117-126.
- 938 Kastens, K., Mascle, J., et al., 1988. ODP Leg 107 in the Tyrrhenian sea: Insights into
939 passive margin and back-arc basin evolution. *Geological Society America Bulletin*, 100,
940 1140-1156.

- 941 Krijgsman, W., Hilgen, F.J., Raffi, I., Sierro, F.J., Wilson, D.S., 1999. Chronology, causes
942 and progression of the Mediterranean salinity crisis. *Nature* 400, 652-655.
- 943 Hilgen, F.J., Kuiper, K., Krijgsman, W., Snel, E., van der Laan, E., 2007. Astronomical
944 tuning as the basis for high resolution chronostratigraphy: the intricate history of the
945 Messinian salinity crisis. *Stratigraphy* 4, 231-238.
- 946 Gennari, R., Manzi, V., Angeletti, L., Bertini, A., Biffi, U., Ceregato, A., Faranda, C.,
947 Gliozzi, E., Lugli, S., Menichetti, E., Rosso, A., Roveri, M., Taviani, M., 2013. A shallow
948 water record of the onset of the Messinian salinity crisis in the Adriatic foredeep
949 (Legnagnone section, Northern Apennines). *Palaeogeography, Palaeoclimatology,*
950 *Palaeoecology*, 386, 145–164.
- 951 Ghielmi, M., Minervini, M., Nini, C., Rogledi, S., Rossi, M., 2013. Late Miocene-Middle
952 Pleistocene sequences in the Po Plain-Northern Adriatic Sea (Italy): the stratigraphic
953 record of modification phases affecting a complex foreland basin. *Marine Petroleum*
954 *Geology*, 42, 50-81.
- 955 Gliozzi, E., Ceci, M.E., Grossi, F., Ligios, S., 2007. Paratethyan Ostracod immigrants in
956 Italy during the Late Miocene. *Geobios*, 40: 325–337.
- 957 Grossi, F., Cosentino, D., Gliozzi, E., 2008. Late Messinian Lago-Mare ostracods and
958 paleoenvironments of the central and eastern Mediterranean Basin. *Boll. Soc. Paleont.*
959 *Ital.* 47, 131–146.
- 960 Gvirtzman Z., Manzi V., Calvo R., Gavireli I., Gennari R., Lugli S., Reghizzi M., Roveri M.,
961 2017. Intra-Messinian truncation surface in the Levant Basin explained by subaqueous
962 dissolution. *Geology*, 45 (10), 915-918.
- 963 Gutscher, M.-A., Kopp, H., Krastel, S., Bohrmann, G., Garlan, T., Zaragosi, S., et al., 2017.
964 Active tectonics of the Calabrian subduction revealed by new multi-beam bathymetric
965 data and high-resolution seismic profiles in the Ionian Sea (Central Mediterranean).
966 *Earth and Planetary Science Letters*, 461, 61–72. [https://doi.org/10.1016/j.](https://doi.org/10.1016/j.epsl.2016.12.020)
967 [epsl.2016.12.020](https://doi.org/10.1016/j.epsl.2016.12.020)
- 968 Iaccarino, S.M., Bertini, A., Di Stefano, A., Ferraro, L., Gennari, R., Grossi, F., Lirer, F.,
969 Manzi, V., Menichetti, E., Ricci Lucchi, M., Taviani, M., Sturiale, G., Angeletti, L., 2008.
970 The Trave section (Monte dei Corvi, Ancona, Central Italy): an integrated
971 paleontological study of the Messinian deposits. *Stratigraphy* 5, 281–306.
- 972 Lofi, J., Gorini, C., Berné, S., Clauzon, G., Tadeu Dos Reis, A., Ryan, W.B.F., Steckler, M.,
973 2005. Erosional processes and paleo-environmental changes in the Western Gulf of
974 Lions (SW France) during the Messinian Salinity Crisis. *Marine Geology* 217, 1-30.
- 975 Lofi, J., 2018. Seismic Atlas of the Messinian salinity crisis markers in the Mediterranean
976 sea. Volume 2 - *Memoires de la Societè Geologique de France*, 181 doi: 10.10682/
977 2018MESSINV2

- 978 Lugli, S., Schreiber, B.C., Triberti, B., 1999. Giant polygons in the Realmontemine
979 (Agrigento, Sicily): evidence for the desiccation of a Messinian halite basin. *Journal of*
980 *Sedimentary Research* 69, 764-771.
- 981 Lugli, S., Bassetti, M.A., Manzi, V., Barbieri, M., Longinelli, A., Roveri, M., 2007. The
982 Messinian "Vena del Gesso" evaporites revisited: characterization of isotopic
983 composition and organic matter. *Geological Society Special Publication* 285, 179–190.
- 984 Lugli, S., Manzi, V., Roveri, M., Schreiber, B.C., 2010. The Primary Lower Gypsum in the
985 Mediterranean: a new facies interpretation for the first stage of the Messinian salinity
986 crisis. *Palaeogeography, Palaeoclimatology, Palaeoecology*, 297, 83–99.
- 987 Madof, A.S, Bertoni, C., Lofi, J., 2019. Discovery of vast fluvial deposits provides evidence
988 for drawdown during the late Miocene Messinian salinity crisis. *Geology*, 47 (2): 171-
989 174.
- 990 Manzi, V., 2001. *Stratigrafia fisica, analisi sedimentologica microscopica e*
991 *caratterizzazione magnetostratigrafica dei depositi connessi all'evento evaporitico del*
992 *Messiniano (Formazione Gessoso-solfifera l.s.). PhD Thesis, University of Bologna*
- 993 Manzi, V., Lugli, S., Ricci Lucchi, F., Roveri, M., 2005. Deep-water clastic evaporites
994 deposition in the Messinian Adriatic foredeep (northern Apennines, Italy): did the
995 Mediterranean ever dry out? *Sedimentology*, 52, 875-902.
- 996 Manzi, V., Roveri, M., Gennari, R., Bertini, A., Biffi, U., Giunta, S., Iaccarino, S.M., Lanci,
997 L., Lugli, S., Negri, A., Riva, A., Rossi, M.E., Taviani, M. (2007) The deep-water
998 counterpart of the Messinian Lower Evaporites in the Apennine foredeep: the
999 Fananello section (Northern Apennines, Italy). *Palaeogeography, Palaeoclimatology,*
1000 *Palaeoecology*, 251, 470-499.
- 1001 Manzi, V., Lugli, S., Roveri, M., Schreiber, B.C., 2009. A new facies model for the Upper
1002 Gypsum (Sicily, Italy): chronological and palaeoenvironmental constraints for the
1003 Messinian salinity crisis in the Mediterranean. *Sedimentology*, 56, 1937–1960.
- 1004 Manzi, V., Lugli, S., Roveri, M., Schreiber, B.C., Gennari, R., 2011. The Messinian
1005 "Calcare di Base" (Sicily, Italy) revisited. *Geological Society of America Bulletin* 123,
1006 347–370.
- 1007 Manzi, V., Gennari, R., Lugli, S., Roveri, M., Scafetta, N., Schreiber, B.C., 2012. High-
1008 frequency cyclicity in the Mediterranean Messinian evaporites: evidence for solar-lunar
1009 climate forcing. *Journal of Sedimentary Research* 82, 991–1005.
- 1010 Manzi, V., Gennari, R., Hilgen, F., Krijgsman, W., Lugli, S., Roveri, M., Sierro, F.J., 2013.
1011 Age refinement of the Messinian salinity crisis onset in the Mediterranean. *Terra Nova*
1012 25, 315-322.

- 1013 Manzi, V., Gennari, R., Lugli, S., Persico, D., Reghizzi, M., Roveri, M., Schreiber, B.C.,
1014 Calvo, R., Gavrieli, I., Gvirtzman, Z., 2018. The onset of the Messinian salinity crisis in
1015 the deep Eastern Mediterranean basin. *Terra Nov.* 38, 42-49.
- 1016 Masetti, D., Fantoni, R., Romano, R., Sartorio, D., Trevisani, E., 2012.
1017 Tectonostratigraphic evolution of the Jurassic extensional basins of the eastern
1018 southern Alps and Adriatic foreland based on an integrated study of surface and
1019 subsurface data. *AAPG Bulletin*, 96/11, 2065–2089.
- 1020 Matano, F., Barbieri, M., Di Nocera, S., Torre, M., 2005. Stratigraphy and strontium
1021 geochemistry of Messinian evaporite-bearing successions of the southern Apennines
1022 foredeep, Italy: implications for the Mediterranean “salinity crisis” and regional
1023 palaeogeography. *Palaeogeography, Palaeoclimatology, Palaeoecology*, 217, 87-114.
- 1024 Matano, F., 2007. Evaporite deposits of the Messinian southern Apennines foreland basin
1025 (Irpinia-Daunia Mts., southern Italy). In: Schreiber, B.C., Lugli, S., Babel, M. (Eds.),
1026 *Evaporites through Space and Time*, Geological Society, London, Special Publications,
1027 285, 165-192.
- 1028 Meilijson, A., Steinberg, J., Hilgen, F., Bialik, O.M., Waldmann, N.D., Makovsky, Y., 2018.
1029 Deep-basin evidence resolves a 50-year-old debate and demonstrates synchronous
1030 onset of Messinian evaporite deposition in a non-desiccated Mediterranean. *Geology*
1031 46, 4–7.
- 1032 Meilijson, A., Hilgen, F., Sepulveda, J., Steinberg, J., Fairbank, V., Flecker, R., Waldmann,
1033 N.D., Spaulding, S.A., Bialik, O.M., Boudinot, F.G., Illner, P., Makovsky, Y., 2019.
1034 Chronology with a pinch of salt: Integrated stratigraphy of Messinian evaporites in the
1035 deep Eastern Mediterranean reveals long-lasting halite deposition during Atlantic
1036 connectivity. *Earth-Science Reviews*, 194, 374-398.
- 1037 Milli, S., Moscatelli M., Stanzione, O., Falcini F., 2007. Sedimentology and physical
1038 stratigraphy of the Messinian turbidite deposits of the Laga Basin (central Apennines,
1039 Italy). *Boll.Soc.Geol.It. (Ital.J.Geosci.)*, 126, 255-281.
- 1040 Ochoa, D., Sierro, F.J., Lofi, J., Maillard, A., Flores, J.A., Suarez, M., 2015. Synchronous
1041 onset of the Messinian evaporite precipitation: First Mediterranean offshore evidence.
1042 *Earth Planetary Science Letters*, 427, 112-124.
- 1043 Ori, G.G., Roveri, M., Vannoni, F., 1986, Plio-Pleistocene sedimentation in the Apenninic-
1044 Adriatic foredeep (central Adriatic Sea, Italy). In: *Foreland Basin* (Ed. By P.A., Allen & P.
1045 Homewood), *Spec. Pub. Int. Ass. Sed.*, 8, 183-198.
- 1046 Orszag-Sperber, F., 2006. Changing perspectives in the concept of “Lago-Mare” in
1047 Mediterranean Late Miocene evolution. *Sedimentary Geology*, 188-189: 259-277.
- 1048 Patacca, E., Scandone, P., 2007. Geology of the Southern Apennines. In: Mazzotti A.,
1049 Patacca E., Scandone P. (Eds.), *Results of the CROP Project, Sub-project CROP-04*
1050 *Southern Apennines (Italy)*, 75–119. *Spec. Issue 7, Boll. Soc. Geol. It. (Ital.J.Geosci.)*.

- 1051 Patacca, E., Scandone, P., 2011. Calabria and Peloritani: Where did they stay before the
1052 Corsica-Sardinia rotation? Boundary conditions, internal geological constraints and first-
1053 order open problems. *Rendiconti online Soc. Geol. It.*, 15, 97-101.
- 1054 Pellen, R., Popescu, S.M., Suc, J.P., Melinte-Dobrinescu M.C., Rubino J.L., Rabineau, M.,
1055 Marabini S., Loget, N., Casero, P., Cavazza, W., Head, M..J., Aslanian, D., 2017. The
1056 Apennine foredeep (Italy) during the latest Messinian: Lago Mare reflects competing
1057 brackish and marine conditions based on calcareous nannofossils and dinoflagellate
1058 cyst. *Geobios.* 50, 237-257.
- 1059 Popescu, S.-M., Melinte-Dobrinescu, M.C., Dalesme, F., Süto-Szentai, M., Jouannic, G.,
1060 Bakrac, K., Escarguel, G., Clauzon, G., Head, M.J., Suc, J.-P., 2009. Galeacysta
1061 Etrusca complex: dinoflagellate cyst marker of paratethyan influxes to the
1062 Mediterranean Sea before and after the Peak of the Messinian Salinity Crisis.
1063 *Palinology* 33, 105–134.
- 1064 Ricci Lucchi, F., 1975. Miocene palaeogeography and basin analysis in the Periadriatic
1065 Apennines. In: *Geology of Italy* (Ed. by C. Squyres), 2, 129-236. PESL, Castelfranco-
1066 Tripoli.
- 1067 Ricci Lucchi, F., 1986, The Oligocene to Holocene foreland basins of the northern
1068 Apennines. In Allen, P.A., and Homewood, P. (Eds.) *Foreland basins: International
1069 Association of Sedimentologists Special Publication 8*, 105-139.
- 1070 Ricci Lucchi, F., Bassetti, M.A., Manzi, V., Roveri, M. (2002) Il Messiniano trent'anni dopo:
1071 eventi connessi alla crisi di salinità nell'avanfossa appenninica. *Studi Geologici Camerti*,
1072 1, 127-142.
- 1073 Rizzini, F., 2005. Il sistema d'avanfossa dell'Appennino settentrionale durante la crisi di
1074 salinità del Messiniano: vincoli tettonostratigrafici per una ricostruzione paleogeografica.
1075 PhD Thesis, University of Parma.
- 1076 Roda, C., 1964. Distribuzione e facies dei sediment neogenici nel Bacino Crotonese.
1077 *Geologica Romana*, 3, 319-366.
- 1078 Rossi, M., Rogledi, S., Barbacini, G., Casadei, D., Iaccarino, S., Papani, G., 2002.
1079 Tectono-stratigraphic architecture of Messinian piggyback basins of northern
1080 Apennines: the Emilia folds in the Reggio-Modena area and comparison with the
1081 Lombardia and Romagna sectors. *Boll. Soc. Geol. It.* 1, 437-447.
- 1082 Rossi M., Minervini M., Ghielmi M., Rogledi S., 2015. Messinian and Pliocene erosional
1083 surfaces in the Po Plain-Adriatic Basin: Insights from allostratigraphy and sequence
1084 stratigraphy in assessing play concepts related to accommodation and gateway
1085 turnarounds in tectonically active margins.
- 1086 Rouchy, J.M., Orszag-Sperber, F., Blanc-Valleron, M.-M., Pierre, C., Rivière, M.,
1087 Combourieu-Nebout, N., Panayides, I., 2001. Paleoenvironmental changes at the

- 1088 Messinian–Pliocene boundary in the eastern Mediterranean (southern Cyprus basins):
1089 significance of the Messinian Lago-Mare. *Sedimentary Geology*, 145: 93-117.
- 1090 Roveri M., Ori G.G., Zitellini N., 1986, Sedimentazione Plio-Quaternaria nell'Adriatico
1091 centrale. In: Atti Riunione Gruppo Sedimentologia, CNR, Ancona, 5-7 giugno 1986,
1092 141-146.
- 1093 Roveri M., Bernasconi A., Rossi M.E., Visentin C., 1992, Sedimentary evolution of the
1094 Luna Field area, Calabria, southern Italy. AGIP SpA-PETER, 20097, S. Donato
1095 Milanese, Milano, Italy.
- 1096 Roveri, M., Manzi, V., Bassetti, M.A., Merini, M., Ricci Lucchi, F., 1998. Stratigraphy of the
1097 Messinian post-evaporitic stage in eastern Romagna (northern Apennines, Italy).
1098 *Giornale di Geologia*, 60, 119-142.
- 1099 Roveri M., Argnani A., Lucente C. C., Manzi V., Ricci Lucchi F. 1999. Guida all'escursione
1100 nelle valli del Marecchia e del Savio. 6 ottobre 1999 Riunione autunnale del Gruppo
1101 Informale di Sedimentologia, Rimini, 3-6 Ottobre 1999.
- 1102 Roveri, M., Bassetti, M.A., Ricci Lucchi, F., 2001. The Mediterranean Messinian salinity
1103 crisis: an Apennine foredeep perspective. *Sediment. Geol.* 140, 201–214.
- 1104 Roveri, M., Manzi, V., Ricci Lucchi, F., & Rogledi, S. (2003). Sedimentary and tectonic
1105 evolution of the Vena del Gesso basin (Northern Apennines, Italy): Implications for the
1106 onset of the Messinian salinity crisis. *Geological Society of America Bulletin*, 115, 387–
1107 405.
- 1108 Roveri M., Boscolo Gallo A. Rossi M.E., Gennari R., Iaccarino S.M., Lugli S., Manzi V.,
1109 Negri A., Rizzini F., Taviani M. (2005) The Adriatic foreland record of Messinian events
1110 (central Adriatic Sea, Italy). *Geoacta*, 4, 139-158.
- 1111 Roveri M., Landuzzi A., Bassetti M.A. Lugli S., Manzi V., Ricci Lucchi F., Vai G.B., 2004.
1112 The record of Messinian events in the northern Apennines foredeep basins. B19 Field
1113 trip guidebook. 32nd International Geological Congress, Firenze, 20-28 Agosto 2004.
- 1114 Roveri, M., Manzi, V., 2006. The Messinian salinity crisis: Looking for a new paradigm?
1115 *Palaeogeography, Palaeoclimatology, Palaeoecology* 238, 386-398.
- 1116 Roveri M., Gennari R., Grossi F., Lugli S., Manzi V., Iaccarino S.M., Taviani M., 2006., The
1117 record of Messinian events in the Northern Apennines foredeep basins. *Acta Naturalia*
1118 *de l'Ateneo Parmense*, 42/3, 47-123.
- 1119 Roveri, M., Lugli, S., Manzi, M., Schreiber, B.C., 2008a. The Messinian Sicilian
1120 stratigraphy revisited: new insights for the Messinian salinity crisis. *Terra Nova* 20, 483–
1121 488.
- 1122 Roveri, M., Lugli, S., Manzi, V., Schreiber, B.C., 2008b. The Messinian salinity crisis: a
1123 sequence-stratigraphic approach. *Geoacta Special Publication* 1, 117–138.

- 1124 Roveri, M., Bertini, A., Cosentino, D., Di Stefano, A., Gennari, R., Gliozzi, E., Grossi, F.,
1125 Iaccarino, S.M., Lugli, S., Manzi, V., Taviani, M., 2008c. A high-resolution stratigraphic
1126 framework for the latest Messinian events in the Mediterranean area. *Stratigraphy* 5,
1127 323–342.
- 1128 Roveri M., Lugli S., Manzi V., Schreiber B.C., 2008d. The shallow- to deep-water record of
1129 the Messinian salinity crisis: New insights from Sicily, Calabria, and Apennine basins, in
1130 Briand, F., *The Messinian Salinity Crisis Mega-Deposits to Microbiology—A Consensus*
1131 *Report: Commission Internationale pour l'Exploration Scientifique de la mer*
1132 *Méditerranée (CIESM) Workshop Monographs*, 33, 73–82.
- 1133 Roveri, M., Lugli, S., Manzi, V., Gennari, R. & Schreiber, B.C. 2014a. High-resolution
1134 strontium isotope stratigraphy of the Messinian deep Mediterranean basins: implications
1135 for marginal to central basins correlation. *Marine Geology*, 349, 113-125.
- 1136 Roveri M., Flecker R., Krijgsman W., Lofi J., Lugli S., Manzi V., Sierro F.J., Bertini A.,
1137 Camerlenghi A., De Lange G., Govers R., Hilgen F.J., Hübscher C., Meijer P.Th., Stoica
1138 M., 2014b. The Messinian Salinity Crisis: past and future of a great challenge for marine
1139 sciences. *Marine Geology*, 352, 25-28.
- 1140 Roveri, M., Manzi, V., Bergamasco, A., Falcieri, F., Gennari, R., Lugli, S. 2014c. Dense
1141 shelf water cascading and Messinian canyons: a new scenario for the Mediterranean
1142 salinity crisis. *American Journal of Science*, 314, 751-784.
- 1143 Roveri M., Gennari, R., Lugli S., Manzi V., Minelli N., Reghizzi M., Riva A., Rossi M.E.,
1144 Schreiber B.C., 2016. The Messinian salinity crisis: open problems and possible
1145 implications for Mediterranean petroleum systems. *Petroleum Geoscience*, 22, 283-290.
- 1146 Roveri M, Gennari R., Ligi M., Lugli S., Manzi V., Reghizzi M., 2019. The synthetic seismic
1147 expression of the Messinian salinity crisis from onshore records: implications for
1148 shallow- to deep-water correlations. *Basin Research*, 31, 1121-1152.
- 1149 Ruggieri, G., 1967. The Miocene and later evolution of the Mediterranean Sea. In: Adams,
1150 C.G., Ager, D.V. (Eds.), *Aspects of Tethyan Biogeography*, vol. 7. Systematics
1151 Association Publication, London, U.K., pp. 283–290. Ryan, W.B.F., Cita, M.B., 1978. The
1152 nature and distribution of Messinian erosion surfaces, indicators of a several-kilometer-
1153 deep Mediterranean in the Miocene. *Marine Geology*, 27/3-4, 193-230.
- 1154 Ruggieri G. 1970 Note Illustrative della Carta Geologica d'Italia alla Scala 1:100.000,
1155 Foglio 108, Mercato Saraceno. Servizio Geologico d'Italia 1-56.
- 1156 Ruggieri G., Torre G., 1984. Il Miocene Superiore di Cozzo Terravecchia, Sicilia Centrale.
1157 *Giornale di Geologia*, 46, 33-43.
- 1158 Sampalmieri, G., Cipollari P., Cosentino, D., Iadanza, A., Lugli, S., Soligo, M., 2008: Le
1159 facies evaporitiche della crisi di salinità messiniana: Radioattività naturale della
1160 Formazione Gessoso-Solfifera della Maiella (Abruzzo, Italia centrale). *Boll. Soc. Geol.*
1161 *Ital.*, 127, 25-36.

- 1162 Sampalmieri, G., Iadanza, A., Cipollari, P., Cosentino D., Lo Mastro, S., 2010.
1163 Paleoenvironments of the Mediterranean Basin at the Messinian hypersaline/hyposaline
1164 transition: Evidence from natural radio activity and micro facies of post-evaporitic
1165 successions of the Adriatic sub-basin. *Terra Nova*, 22, 239-250
- 1166 Santantonio, M., Scrocca, D., Lipparini, L., 2013. The Ombrina-Rospo Plateau (Apulian
1167 Platform): Evolution of a Carbonate Platform and its Margins during the Jurassic and
1168 Cretaceous. *Marine and Petroleum Geology*, 42, 4-29.
- 1169 Sierro, F.J., Flores, J.A., Zamarréño, I., Vazquez, A., Utrilla, R., Frances, G., Hilgen, F.J.,
1170 Krijgsman, W., 1999. Messinian pre-evaporite sapropels and precession-induced
1171 oscillations in western Mediterranean climate. *Marine Geology* 153, 137-146.
- 1172 Trincardi, F., and Argnani, A., 2001. Carta Geologica dei Mari Italiani alla scala 1:250000:
1173 Foglio JOG NL33-10 "Ravenna", ISPRA – Servizio Geologico d'Italia., Selca, Firenze.
- 1174 Trincardi, F., Argnani, A., Coreggiari, A., 2011a. Carta Geologica dei Mari Italiani alla scala
1175 1:250:000. Foglio NL33-7 Venezia, ISPRA - Servizio Geologico d'Italia, Selca, Firenze.
- 1176 Trincardi, F., Argnani, A., Coreggiari, A., 2011b. Carta Geologica dei Mari Italiani alla scala
1177 1:250:000. Foglio NK33-1/2 Ancona, ISPRA - Servizio Geologico d'Italia, Selca,
1178 Firenze.
- 1179 Trincardi, F., Argnani, A., Coreggiari, A., 2011c. Carta Geologica dei Mari Italiani alla scala
1180 1:250:000. Foglio NK33-5 Pescara, , ISPRA - Servizio Geologico d'Italia, Selca,
1181 Firenze.
- 1182 Trincardi, F., Argnani, A., Coreggiari, A., 2011d. Carta Geologica dei Mari Italiani alla scala
1183 1:250:000. Foglio NK33-6 Vieste, ISPRA - Servizio Geologico d'Italia, Selca, Firenze.
- 1184 Trincardi, F., Argnani, A., Coreggiari, A., 2011e. Carta Geologica dei Mari Italiani alla scala
1185 1:250:000. Foglio NK33-8/9 Bari, ISPRA - Servizio Geologico d'Italia, Selca, Firenze.
- 1186 Trua, T., Manzi, V., Roveri, M., Artoni, A., 2010. The Messinian volcanoclastic layers of the
1187 Northern Apennines: evidence for the initial phases of the Southern Tyrrhenian
1188 spreading? *Ital.J.Geosci.*, 129-2, 269-279,
- 1189 Vai, G.B., 1988. A field trip guide to the Romagna Apennine geology: the Lamone valley.
1190 In: De Giuli, C., Vai, G.B. (Eds.), *Fossil Vertebrates in the Lamone Valley, Romagna*
1191 *Apennines, Int. Work. Continental Faunas at the Miocene/Pliocene Boundary*, pp. 7–37.
- 1192 Vai, G.B., 1997. Cyclostratigraphic estimate of the Messinian Stage duration. In:
1193 Montanari, A., Odin, G.S., Coccioni, R. (Eds.), *Miocene Stratigraphy: An Integrated*
1194 *Approach. Developments in Paleontology and Stratigraphy*, 15, pp. 463–476.
- 1195 Vai, G.B., 2016. Over half a century of Messinian salinity crisis. *Boletín Geológico y*
1196 *Minero*, 127 (2/3), 615-632.
- 1197 Van Couvering, J.A., Castradori, D., Cita, M.B., Hilgen, F.J. and Rio, D., 2000. The base of
1198 the Zanclean Stage and of the Pliocene Series. *Episodes*, 23–3, 179–187.

- 1199 Van Dijk, J.P., Bello M., Brancaleoni G.P., Cantarella G., Costa V., Frixia A., Golfetto F.,
 1200 Merlini S., Riva M., Torricelli S., Toscano C., Zerilli A., 2000. A regional structural model
 1201 for the northern sector of the Calabrian Arc (southern Italy). *Tectonophysics*, 324, 267-
 1202 320.
- 1203 Vasiliev, I., Lugli, S., Reichart, G.J., Manzi V., Roveri, M., 2017. How dry was the
 1204 Mediterranean during the Messinian salinity crisis? *Palaeogeography*,
 1205 *Palaeoclimatology*, *Palaeoecology*, 471, 120–133.
- 1206 Vitale, S., Ciarcia, S., 2013: Tectono-stratigraphic and kinematic evolution of the southern
 1207 Apennines/Calabria-Peloritani Terrane system (Italy). *Tectonophysics*, 538, 164-182.
- 1208 Wrigley R., Hodgson N., Esestime P., 2015. Petroleum geology and hydrocarbon potential
 1209 of the Adriatic basin, offshore Croatia. *Journal of Petroleum Geology*, 38/3, 301-316.
- 1210 Zecchin M., Massari F., Mellere G., Prosser G., 2003. Architectural styles of prograding
 1211 wedges in a tectonically active setting, Crotona Basin, Southern Italy. *J. Geol. Soc.*
 1212 *Lond.*, 160, 863-880.

1213

1214 **Figure captions**

1215

1216 **Fig.1.** A) Geological map of the Central and Southern Apennines and, in the inset (B), a
 1217 schematic structural map of Italy. The map includes: i) the location of the boreholes used
 1218 for this study; ii) **the main MSC basins**, both outcropping (after Manzi, 2001; Roveri et al.,
 1219 2003; Manzi et al., 2005; Roveri et al., 2006) and buried under the Po plain (after Manzi,
 1220 2001; Roveri et al., 2003; Rizzini, 2005; Ghielmi et al., 2013; Rossi et al., 2015); iii) the
 1221 extension in the Adriatic offshore of the MSC deposits (modified from CNR map) below the
 1222 Pliocene units; iv) the main tectonic structures (modified from CNR map); v) the main
 1223 diapirs of Triassic evaporites and the distribution of the Dalmatian Mesozoic Platform
 1224 deposit (modified after Wrigley et al., 2015); vi) the extension in the Adriatic offshore of the
 1225 MSC deposits (modified from CNR map) below the Pliocene units; vii) the location of the
 1226 boreholes used for this study.

1227 The main **MSC basins**, both outcropping (after Manzi, 2001; Roveri et al., 2003; Manzi et
 1228 al., 2005; Roveri et al., 2006) and buried under the Po plain (after Manzi, 2001; Roveri et
 1229 al., 2003; Rizzini, 2005; Ghielmi et al., 2013; Rossi et al., 2015). Two types can be
 1230 distinguished. **PLG basins** - basins that hosted the deposition of shallow water primary
 1231 evaporites (PLG unit) during stage 1: Epiligurian (E), Emilia-Veneto (EV), Vena del Gesso
 1232 (VdG), Val Marecchia (VM), Molise (M), Maiella (MA), Irpinia (I), Adriatic (A). **RLG basins** -
 1233 those where only clastic evaporites (RLG unit) were deposited during stage 2: Messinian

1234 main foredeep (MF), Eastern Romagna (ER), Northern Marche (NM), Laga (L), Bradanic
 1235 Trough (B), Sibari-Rossano (S), Crotone basins (K), South Adriatic Basin (SAB).
 1236 The main **tectonic features** are: Apennines buried thrust front (ABTF), Livorno Sillaro line
 1237 (LS), Forlì Line (FL), Val Marecchia line (VM), Sibillini Mountains thrust line (SM), Olevano-
 1238 Antrodoco line (OA), Chienti Line (C), Gran Sasso thrust front (GS), Maiella Rocca
 1239 Monfina line (MRM), Gargano high (G), Murge high (M), Sangineto line (SG).
 1240 The main **tectonic units/domains**: Ligurian units (L), Tuscan unit (T), Macigno-Cervarola
 1241 unit (MC), Inner Umbro-Marchean units (IUM), Outer Umbro-Marchean units (OUM),
 1242 Lazio-Abruzzi platforms (LAP), Molise-Lagonegro nappes (MLN), Bradanic Trough (BT),
 1243 Calabrian Arc (CA), Apulian Mesozoic platform (AP), Dalmatian Mesozoic Platform (DP),
 1244 Dinaric units (DU).

1245

1246 **Fig. 2.** Outcrop examples of the MSC evaporites. A) the PLG unit forms an up 200 m-
 1247 thick tabular body with strong lateral persistence. (Vena del Gesso, between the Sgarba
 1248 stream and the Senio river). The location of the Monte Tondo quarry and Spes quarry
 1249 sections, where the reference PLG sections have been measured by Lugli et al. (2010),
 1250 are reported. Photo, courtesy of Piero Lucci; B) closer view of the Monte del Casino area
 1251 shown in A, notice the thickest beds of the lower PLG cycles (PLG3 partially covered by
 1252 the vegetation, PLG4, PLG5, PLG6). Photo, courtesy of P. Lucci; C) example of the RLG
 1253 unit (left side of the Lese river valley, Crotone basin) consisting of alternation of hybrid
 1254 carbonate-gypsum clastic turbidites and shale resting on top of the Ponda Fm (badlands).
 1255 B and C are reported at the same scale to allow the immediate comparison between the
 1256 PLG showing thicker beds separated by very thin shale beds (B) and the RLG where
 1257 thinner beds are intercalated by shale intervals of similar thickness (C).

1258

1259 **Fig. 3.** Outcrop examples of the MSC evaporites. A) a normal fault in the PLG unit close
 1260 to the Spes quarry (fig. 2) allow a direct comparison between the lower and the upper PLG
 1261 gypsum beds. Notice the homogeneous aspect of the cycles PLG3-5 made up by the
 1262 massive and banded selenite facies only. B) Closer view of cycle PLG8 and PLG9 (base;
 1263 Monte Tondo quarry). Notice that the lower part of the bed consisting of massive selenite
 1264 is more resistant to the weathering of the upper part of the cycle consisting of branching
 1265 selenite. C) turbiditic gypsarenite beds (ga) alternated to dark organic-rich shale (s). B and
 1266 C are reported at the same scale to allow the immediate comparison between the PLG

1267 showing thicker beds separated by very thin shale beds (B) and the RLG where thinner
1268 beds are intercalated by shale intervals (C).

1269

1270 **Fig. 4.** A) Location of the ViDEPI boreholes in the study area; in black the available
1271 boreholes; in yellow those that cross the MSC deposits resting above the Autochthonous
1272 domain; in red the boreholes that are were drilled above the Translated Allochthonous
1273 Domain (see the trace of the front of the allochthonous). B) distribution of the different
1274 facies deposited during the Tortonian-Messinian interval, preceding the salinity crisis
1275 onset. The siliciclastic deposition is limited to two area, one in the northern Apennines
1276 foredeep and one above the Calabrian Arc. Elsewhere the hemipelagic deposition is
1277 prevalent, Notice the presence of shallow water carbonate in a small area between the
1278 Gargano and the Gran Sasso. C) distribution of the different facies deposited during stage
1279 1. The PLG deposition occurred mainly in the foreland area in the Adriatic offshore. Minor
1280 basins were located in the inner foredeep (VdG, Vena del Gesso basin), and in the
1281 foreland (now buried below the Po plain). D) distribution of the different facies deposited
1282 during the post-evaporitic interval (stage 2 and 3). Notice that the halite was deposited
1283 only above the allochthonous units of the Calabrian Arc.

1284

1285 **Fig. 5.** Cross section of the PLG unit in the Adriatic offshore. The separation line
1286 between the different cycles (PLG1-2, PLG3-5 and PLG6-16) has been used for
1287 correlation.

1288

1289 **Fig. 6.** Isopach maps of the PLG unit showing the general distribution in the study area
1290 (A) and the detail in the Adriatic offshore focusing on the thickness of the PLG1+2 (B),
1291 PLG3 (C) and PLG4 (D) cycles. Notice as the thickness of the single beds increase in the
1292 eastern (close to the Adriatic midline) and in the south-western (close to the Molise and
1293 Gargano coastline) part of the basin. Modified after Corcagnani, 2017.

1294

1295 **Fig. 7.** Regional scale cross sections showing the distribution of the MSC deposits in
1296 the Adriatic Foredeep and in above the Allochthonous. A) N-S oriented section showing
1297 that the areas were PLG (to the north) and RLG (to the south) evaporites were deposited
1298 is separated by an area with pre-MSC carbonate deposits. Other PLG deposits are found
1299 above at the front of the Allochthonous nappe. B) W-E section showing the RLG unit found

1300 below the Allochthonous; its distribution is limited to the east by a tectonic slope affecting
 1301 the Apula Mesozoic units. These onlap can be better observed in the seismic (C)

1302

1303 **Fig. 8.** Distribution of the Messinian evaporites in the Basilicata area representing the
 1304 northernmost extension of the salt deposits. The RLG units including also gypsum is found
 1305 at the front of the Allochthonous unit only whereas no MSC deposits are found above
 1306 Apula. All the seismic lines cited in the figure and the logs of the boreholes are available
 1307 from <http://www.videpi.com/videpi/videpi.asp>.

1308

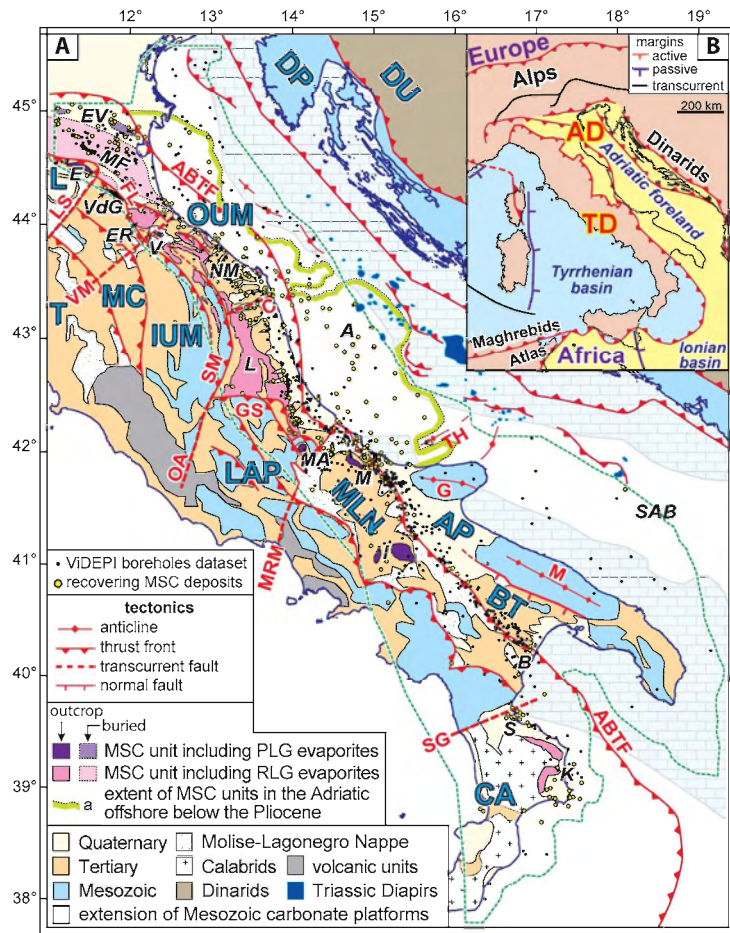
1309 **Fig. 9.** A) Map of the distribution of the Messinian evaporite facies with location of the
 1310 regional seismic sections (B and C) across the Apennines foredeep. Section B is traced in
 1311 the Northern Apennines from the Vena del Gesso basin (VdG) to the Veneto foreland
 1312 (modified after Roveri et al., 2003 and Fantoni et al., 2010; Masetti et al., 2012). Section C
 1313 is traced in the central Apennines from the Laga basin to the Adriatic offshore (Modified
 1314 from Bigi et al., 2009 and Wrigley et al., 2015). The seismic profiles cited in blue are and
 1315 the logs of the boreholes are available from <http://www.videpi.com/videpi/videpi.asp>.
 1316 Notice that: i) the distribution of the PLG evaporites during stage 1 limited to the more
 1317 elevated structural basins in the Apenninic chain and in the foreland (in section B),
 1318 whereas in the foredeep the stage 1 of the crisis is recorded by organic-rich shales (Manzi
 1319 et al., 2007); ii) the hiatus associated with the MES (section C) progressively reduces
 1320 moving westward into the Laga depocenter and a possible MES-cc can be envisaged
 1321 below the gypsarenites belonging to the Evaporitic Member of the Laga Formation (Manzi et
 1322 al., 2005; Milli et al., 2007). RA, Riolo Anticline; BST, Budrio-Selva Thrust; TT, Tresigallo
 1323 Thrust; FT, Ferrara Thrust; AA, Acquasanta Anticline; MTF, Montagna dei Fiori Thrust; BT,
 1324 Bellante Thrust; CS, Costal Structure. The stage 2 + 3 interval crossed by boreholes may
 1325 be recorded exclusively by siliciclastic (s) deposits or may include also resedimented
 1326 gypsum deposits (g), commonly found at the base.

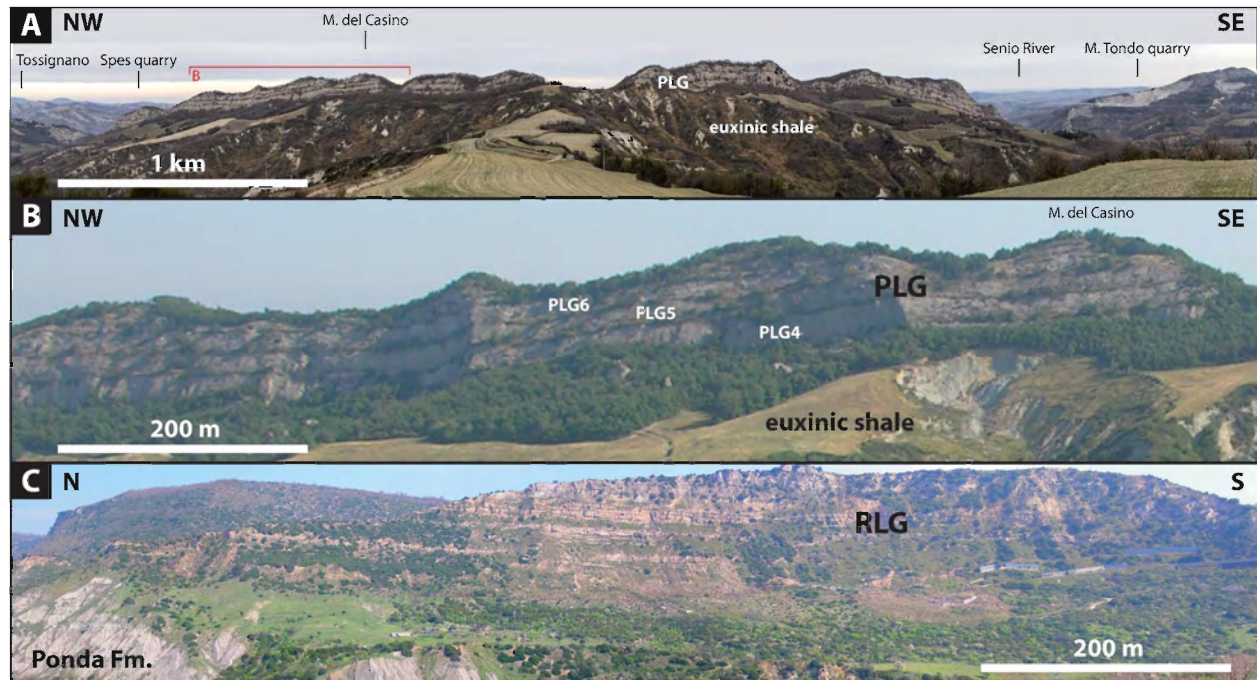
1327

1328 **Fig. 10.** Paleogeographic map of the Central Mediterranean during the stage 2 of the
 1329 Messinian salinity crisis showing the distribution of the paleogeographic domains and the
 1330 main sedimentary facies. The distribution of the PLG (stage 1) in the foreland region is
 1331 also indicated. The dark gray patten in the Adriatic represents a sill separating the southern
 1332 and central-northern basin. The front of the Apennine accretionary wedge is marked in red
 1333 (line with triangles), whereas the Apennine front is in black. The tentative route of clastic

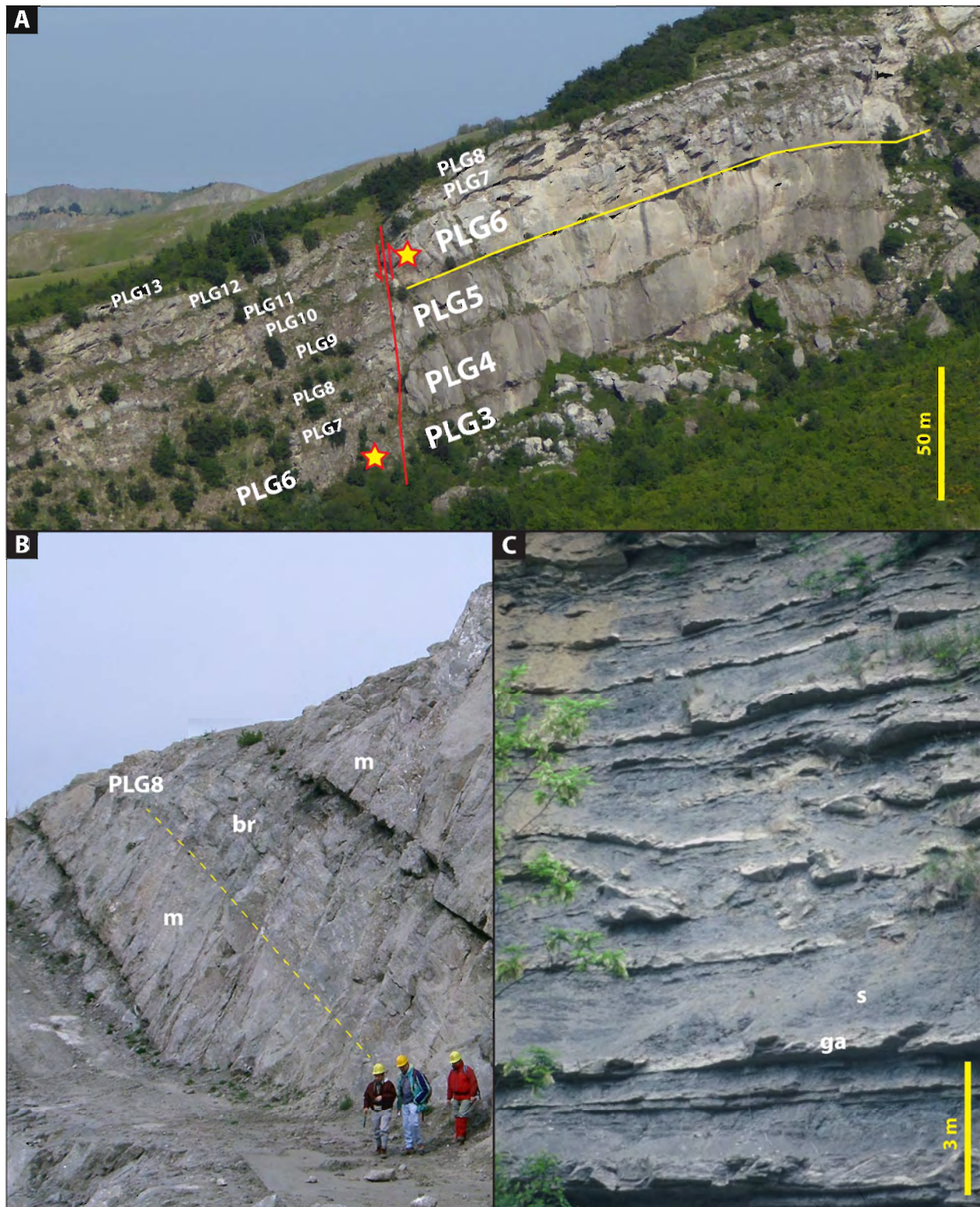
1334 gypsum transport (black arrows) and the flow of brines (red arrows) are also indicated.
1335 Main basins: VdG, Vena del Gesso; A, Adriatic; K, Crotona; T, Tyrrhenian; AP, Algero-
1336 Provençal; C, Caltanissetta; H, Hyblean; I, Irpinian; B, Basilicata Ionian. Modified from
1337 Argnani 2000; 2005; Manzi et al., 2005; Fauquette et al., 2015.

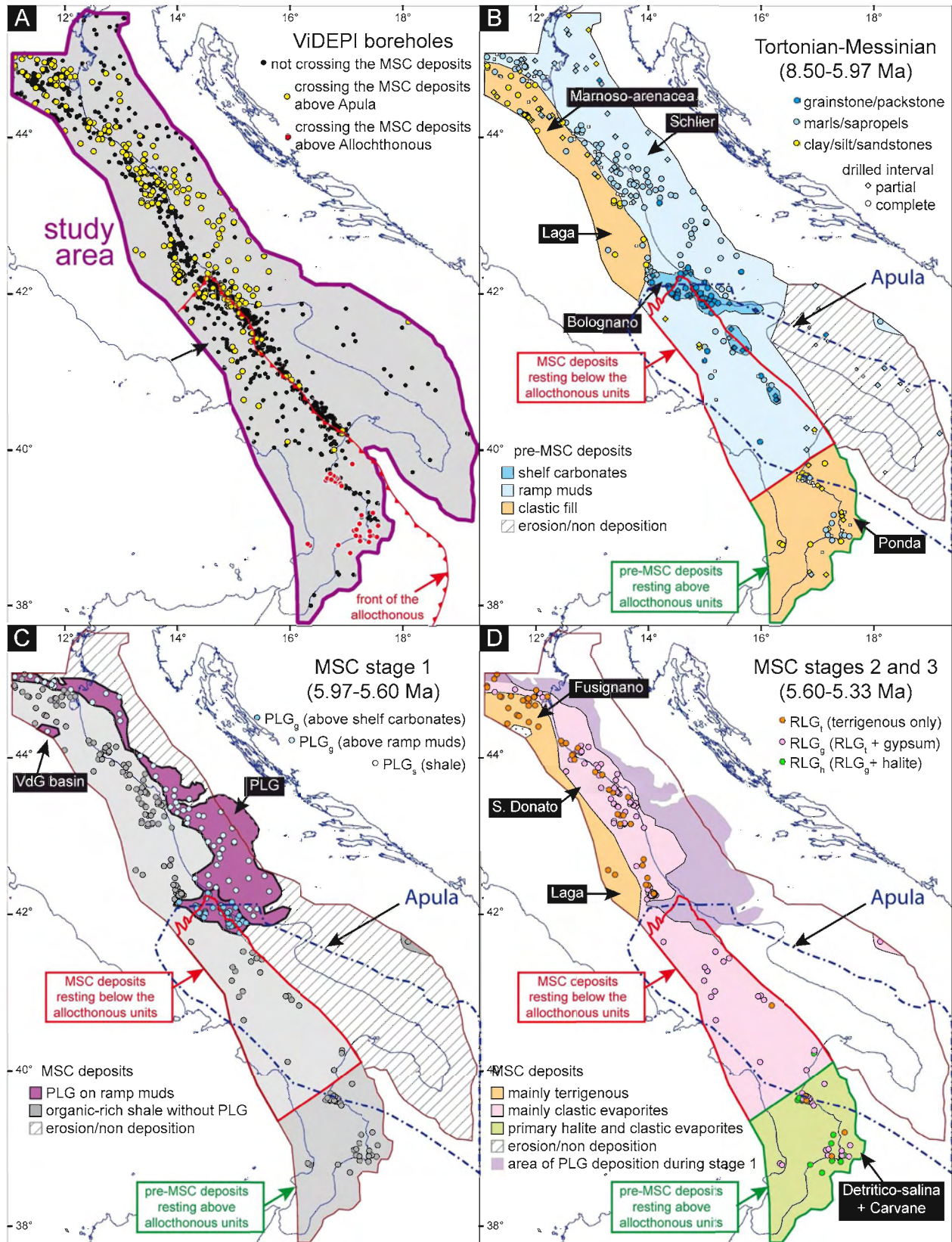
Journal Pre-proof

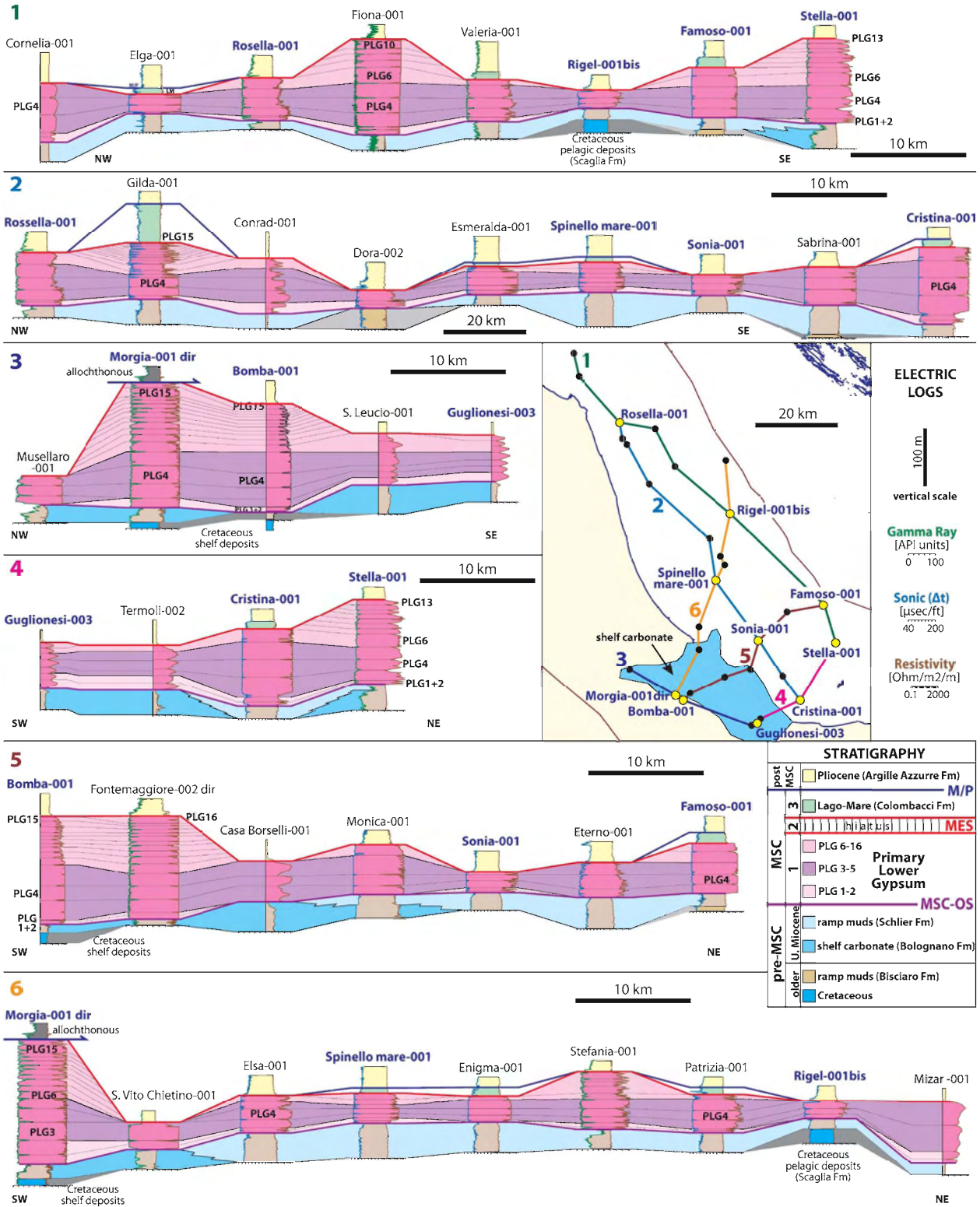


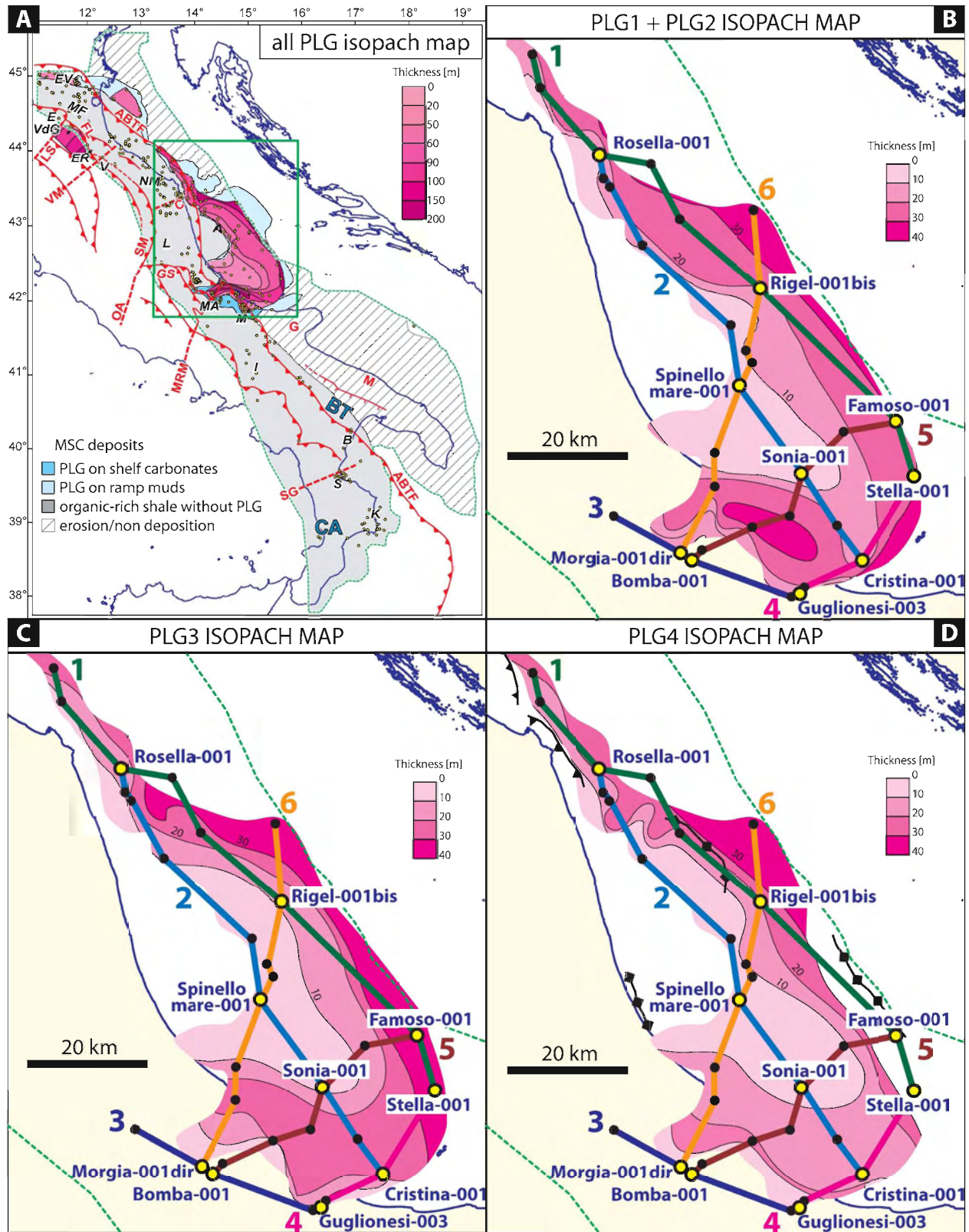


Journal Pre-proof





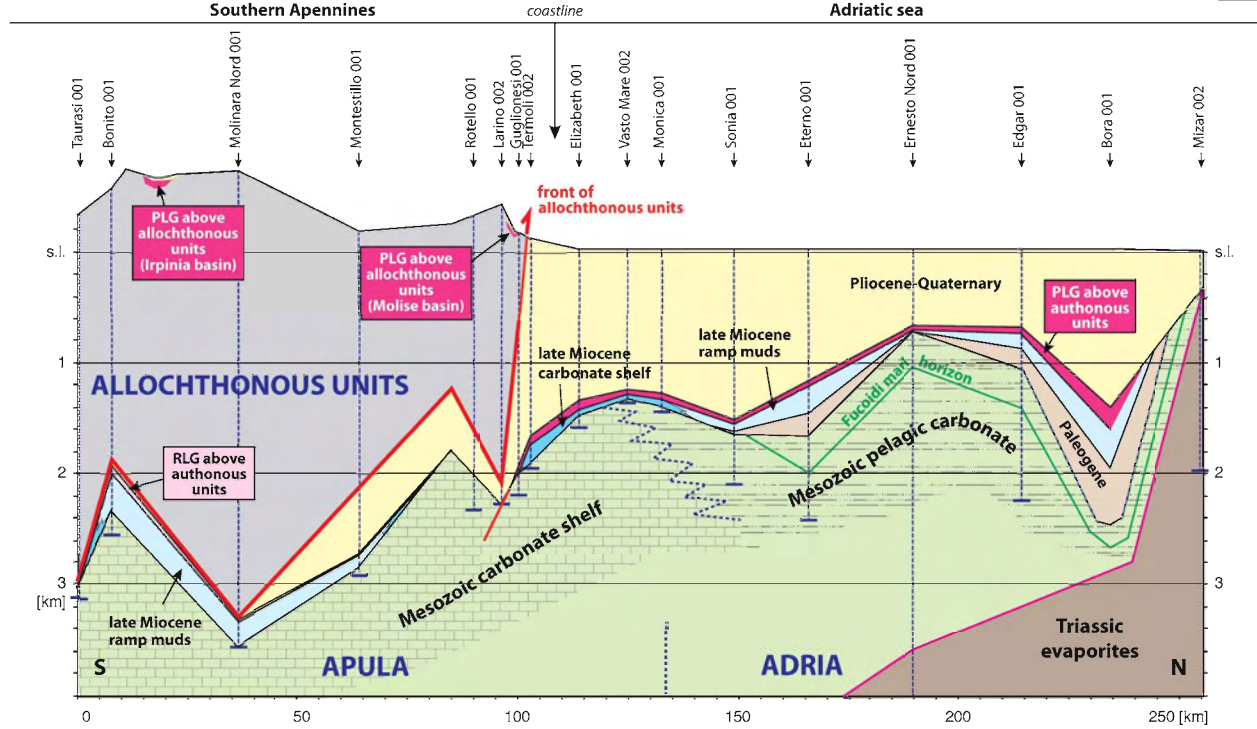




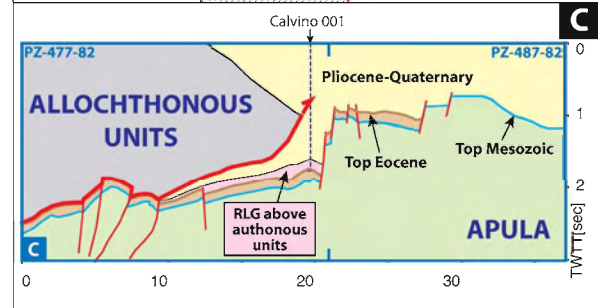
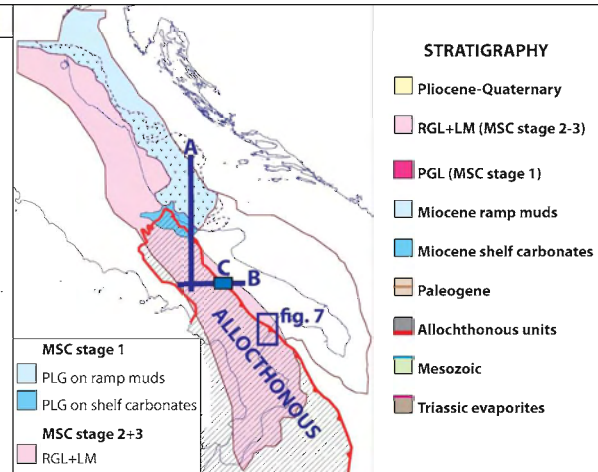
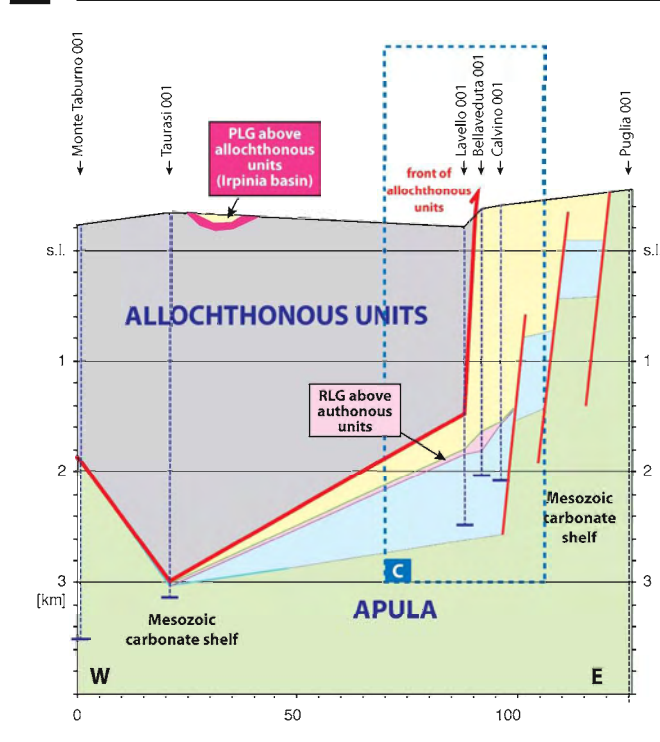
WEDGE-TOP + FOREDEEP BASINS

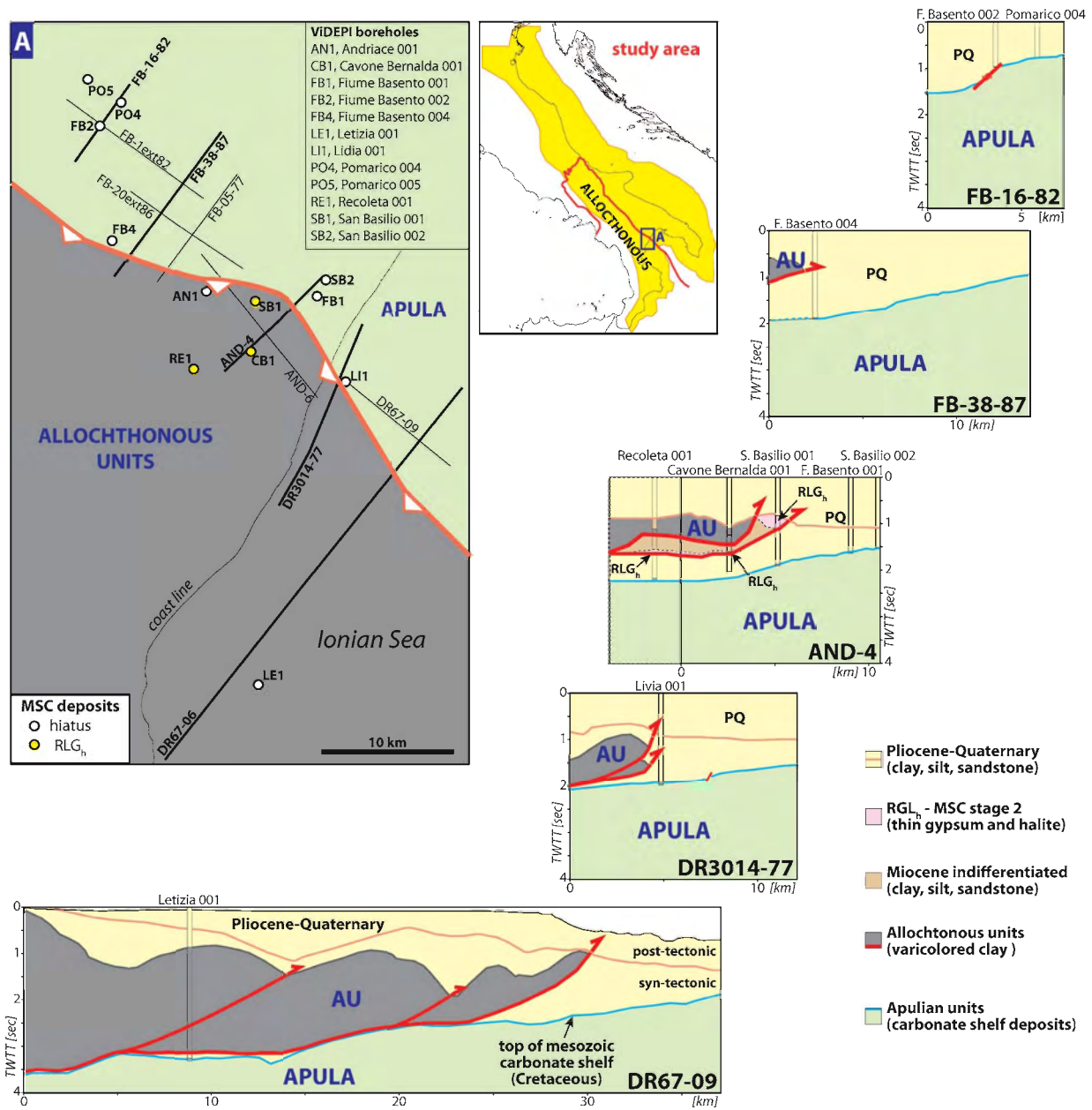
FORELAND + BACKBULGE BASIN

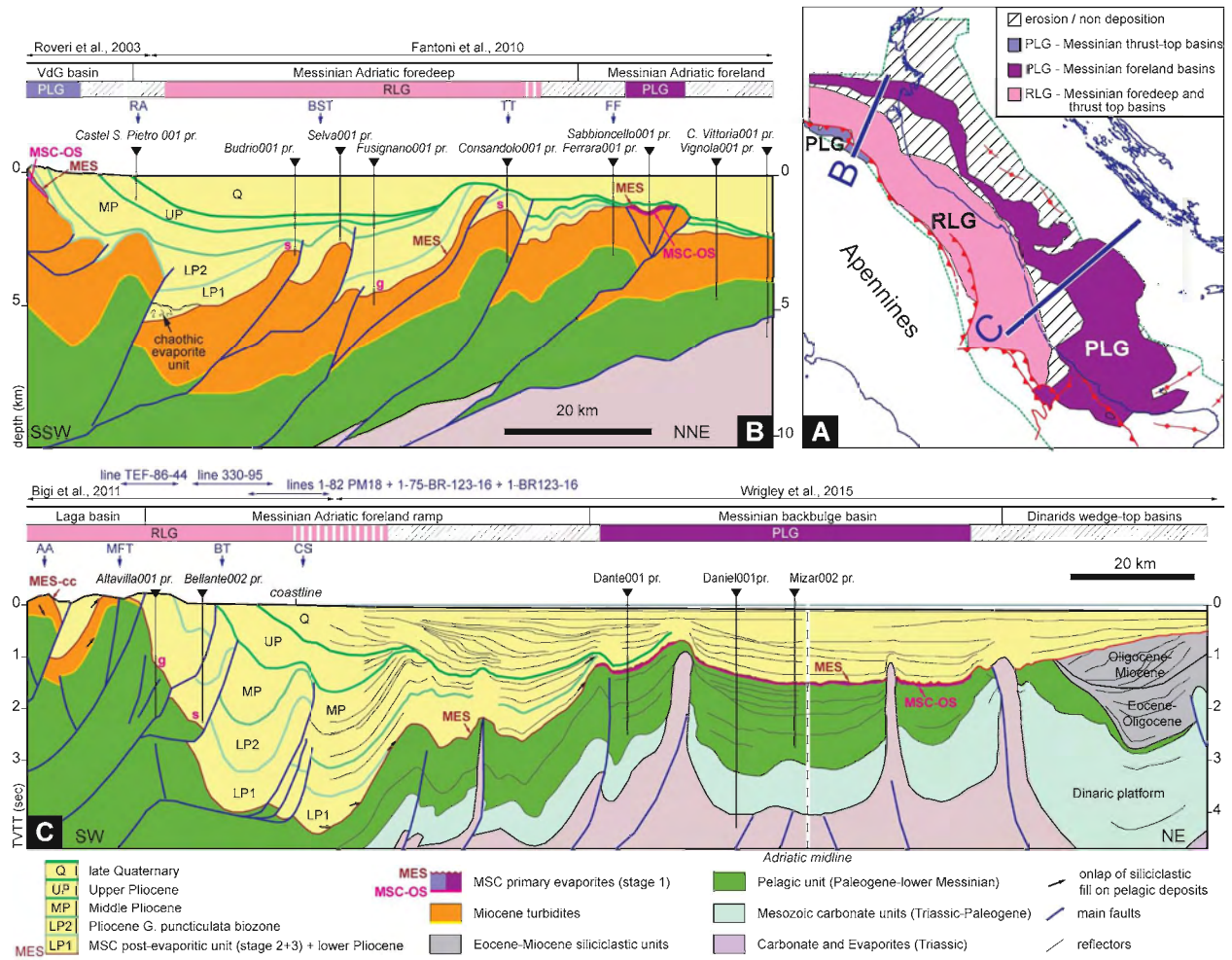
A

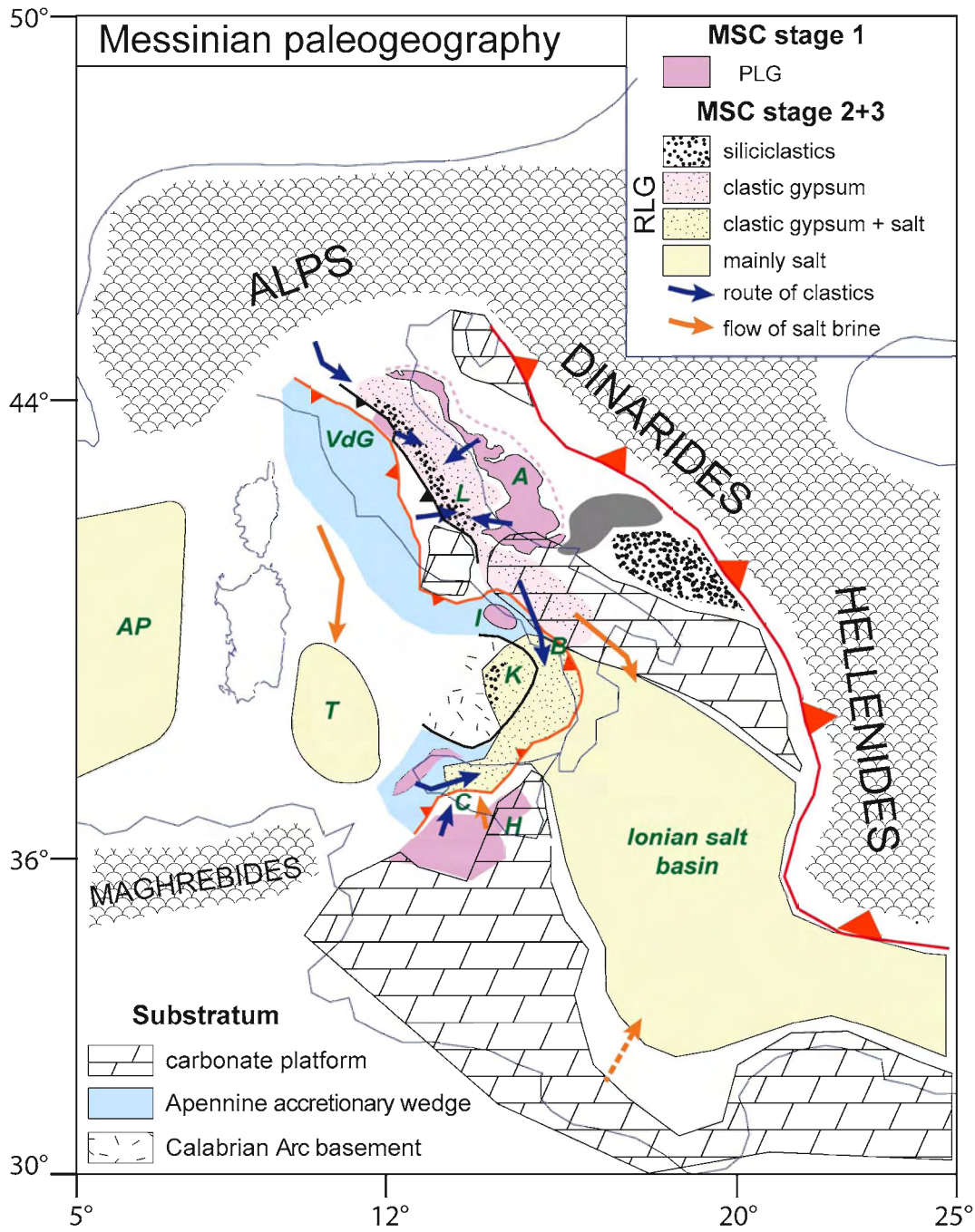


B BRADANIC TROUGH MURGE HIGH









- integration of outcrop and subsurface data led to depict the Messinian salinity crisis in the Adriatic foreland basin;
- the largest evaporitic basin ever described in the Mediterranean was located in the Adriatic foreland
- the distribution of evaporitic facies is a key to reconstruct the evolution of the Apennines

Journal Pre-proof

Declaration of interests

The authors declare that they have no known competing financial interests or personal relationships that could have appeared to influence the work reported in this paper.

The authors declare the following financial interests/personal relationships which may be considered as potential competing interests:

The Authors

Vinicio Manzi, Andrea Argnani, Alessandro Corcagnani, Stefano Lugli, Marco Roveri